



Center for Social Research and Data Archives,  
Institute of Social Science, The University of Tokyo




CSRDA supports the Sustainable Development Goals

SUSTAINABLE  
DEVELOPMENT  
GOALS

# CSRDA Discussion Paper

## Residential Agglomeration of the Homeless and its Effects on Their Living Standards



No. <b>10</b>	Date <b>May. 2023</b>	SDGs   
Name <b>Mariko Nakagawa, Kotaro Iizuka</b>		

# Residential Agglomeration of the Homeless and its Effects on Their Living Standards <sup>\*</sup>

Mariko Nakagawa<sup>†</sup>

Kotaro Iizuka<sup>‡</sup>

May 1, 2023

## Abstract

This research analyzes the benefits enjoyed by homeless persons located on the riverbank of the Tama River near Tokyo when they reside in clusters. To conduct this research, we first detected the housing locations of homeless persons using an unmanned aerial system—a drone—and determined the number of house clusters based on single-linkage clustering, a hierarchical cluster-analysis method. After detecting clusters, we evaluated the effect of residing in a larger cluster on a homeless person’s standard of living, which we quantified by the temperature of each house in winter. Our results show that the larger the cluster in which a house is located, the higher its temperature, indicating that living in a larger cluster improves living standards. In addition, we conducted a thermal experiment in which we built a replica of a typical house in the study area and collected indoor temperature data to supplement that calculated based on drone thermal imaging. The two house temperatures, indoor and drone temperatures, collected during the experiment validate the reliability of the actual data used in the analysis. The finding in this paper suggests the possibility that homeless persons in the study area benefit from living in larger communities via interactions with those living in the same cluster.

---

<sup>\*</sup>The authors are grateful to Naoya Fujiwara, Vernon Henderson, Hirokazu Ishise, Ryo Itoh, Keisuke Kawata, Tatsuhito Kono, Kentaro Nakajima, Ryosuke Okamoto, Yukiko Saito, Yasuhiro Sato, Masayuki Sawada, Takatoshi Tabuchi, Takaaki Takahashi, Kohei Takeda, Kensuke Teshima, David Weil, Atsushi Yamagishi and Dao-Zhi Zeng for their thoughtful comments and suggestions. We would also like to thank seminar participants at the Urban Economics Workshop at the University of Tokyo, the Regional Science Workshop at Tohoku University, OLS seminar at Osaka University, Economic Development Workshop at Hitotsubashi University, and Kansai Labor Workshop. We appreciate the outstanding research assistance of Toshikazu Fukuba, Shungo Itoh, Tomoki Ohira, Chikara Shiba, and Hiroyuki Yamauchi, and we are grateful to Nairu Kimura for sharing his experience staying in the study area. All remaining errors are our own.

<sup>†</sup>Institute of Economic Research, Hitotsubashi University and Graduate School of Information Sciences, Tohoku University. E-mail: nakagawam@ier.hit-u.ac.jp.

<sup>‡</sup>Center for Spatial Information Science, University of Tokyo. E-mail: kiizuka@csis.u-tokyo.ac.jp.

# 1 Introduction

People tend to interact more with those located nearby. More active social interactions are associated with geographic proximity and engender benefits from interaction with others without the costs that stem from interacting over long distances. Marmaros and Sacerdote (2006) examine the likelihood of social interaction among students at Dartmouth College and found that geographic proximity matters when explaining the extent of interaction among students. Using data on adolescents in the United States, Kim et al. (2017) argue that greater geographic dispersion lessens people’s incentives to interact socially.

In the context of the labor market, Bayer et al. (2008) show that individuals residing in the same city block in the Boston metropolitan area were more likely to work together than with those in nearby blocks. Under the assumption that job information is exchanged among agents residing in the same census block, they interpret the result as an outcome of a referral effect and conclude that the findings are evidence of the existence of significant social interactions at the block level. Using detailed geographic employer-employee data from the United States, Schmutte (2015) finds that workers are disproportionately more likely to become coworkers with their neighbors when changing jobs. Additionally, individuals are more likely to become employed at a high-wage firm when their neighbors are already employed at high-wage firms. The author concludes that the role of social networks is important when connecting workers to jobs offered by firms paying high wages.

Geographic proximity plays a pivotal role in enhancing social interactions and benefits relevant agents. These examples indicate how beneficial social networks within a geographic range, in which individuals can reach others, facilitate friendship formation and job searches.

Based on the idea that people benefit from social interactions within geographic proximity, this paper analyzes whether social network benefits can be observed in squatter communities in Japan. Squatter communities have been created on the riverbank of the Tama River near Tokyo, Japan (the study area for this paper). Such urban squatters are usually called “homeless” persons in Japan; indeed, they are classified as homeless in Japan’s municipality reports.<sup>1</sup> Homeless persons in this area usually earn a meager amount of money.<sup>2</sup> and often engage in illicit daily work that incorporates informal information (see Section 2). Since access to such informal information is possible via direct

---

<sup>1</sup>Agglomeration of the homeless is not a phenomenon limited to our study area. Iwata and Karato (2011) find that homeless persons in Osaka, Japan, tend to agglomerate at the city-block level.

<sup>2</sup>Homeless persons in this area rarely beg for money or food and earn money on their own (Division of Health & Welfare in Kawasaki City, 2019; Okamoto, 2007), so the diffusion of informal job-related information is important for increasing their income.

contacts and interactions with other homeless persons, social networks associated with geographic proximity are essential for their lives. Moreover, because their daily incomes tend to be unstable, mutual support through shared food or electromechanical devices stabilizes and enriches their lives.<sup>3</sup> Hence, interaction within a homeless community is expected to be a vital benefit of social networks.

This paper focuses on the benefits derived from agglomeration of homeless persons and examines whether living in a cluster on the bank of the Tama River, which divides Tokyo Prefecture and Kanagawa Prefecture in Japan, improves their living standards. The goal of this paper is to corroborate the existence of a positive agglomeration effect in a society of homeless persons.<sup>4</sup> Specifically, we investigate whether having interactions with more homeless persons leads to higher living standards. However, accomplishing this goal requires overcoming two main obstacles: (i) difficulty detecting interactions among homeless persons associated with geographic proximity and (ii) difficulty defining homeless persons' actual living standards.

The first obstacle stems from the fact that we usually cannot observe who interacts with whom among homeless persons because they lack fixed residential addresses. However, homeless persons in our study area are not nomadic but settled in fixed locations; they build cage-like houses in which they reside and illicitly occupy public land along the riverbank. The exteriors of their houses have typical features; examining the exterior characteristics, we can detect house-like objects in aerial images. By conducting unmanned aerial system (usually called "drone") flights, we can obtain aerial images of our study area. Then, we can use these images to create house-location data<sup>5</sup> on which basis, we can calculate the distance between houses to obtain information about geographic proximity among homeless persons, which can be considered a proxy for their social interactions.

The second obstacle is the difficulty eliciting reliable information from homeless persons. Interviewing homeless individuals is challenging, even when investigators or interviewers can contact them. As is true elsewhere, in Japan, there is a high prevalence of certain mental disorders, including alcohol

---

<sup>3</sup>In the study area, not a few homeless persons own electromechanical devices (Murata, 2015). For more details, see Section 2.

<sup>4</sup>Mechanisms of the agglomeration of homeless persons other than social interaction benefits can be considered. Homeless persons may gravitate to services such as shelters, meal programs, and medical clinics, which induce homeless agglomeration (Culhane, 2010; Corinth and Lucas, 2018; Lee and Price-Spratlen, 2004). Our study, however, does not examine this aspect as such services are not typically offered on the riverbank in our study area. There are no facilities such as soup kitchens or shelters on the riverbank, and it is rare for food banks to provide free food services there. According to our interview with the Division of the Medial Welfare Services of Kawasaki City, only three food distribution events were held each month during our study period, which suggests that this mechanism likely does not contribute to the concentration of homeless persons.

<sup>5</sup>There is a demographic tendency for homeless persons in Japan to be single males, which leads to the assumption that each house is occupied by only one homeless person; thus, each house location can be considered the geographic location of a single homeless person. For details, see Section 2.

addiction, among homeless persons. Additionally, some individuals may have a low IQ. Mental and intellectual challenges make it difficult for investigators and interviewers to obtain accurate information about living standards. To overcome this issue, we utilize house temperature data on winter nights as a proxy for residents' living standards.

In our study area, several homeless persons are known to have electronic generators that they can use to operate microwaves, rice cookers, television sets, and heaters. These electrical appliances generate heat when used, and the temperature of a house of a homeless person who is sufficiently well-off to own multiple electrical devices is expected to be higher. Moreover, in the winter, individuals may use heaters to fend off the cold if they can afford to, which also raises the house temperature. Thus, we conjecture that house temperature can be used as a proxy resident affluence.

After identifying house locations, we can obtain house temperature data via a drone loaded with a thermal sensor to obtain thermal images. From these thermal images, we can extract temperature information of the areas overlapping the house polygons and attach the extracted temperature values to each house.<sup>6</sup> The house temperature data sensed by the thermal camera capture the heat that leaks from the houses.

Moreover, to validate the thermal data we collected, we conducted a replication experiment in a private drone field by temporarily building a simple-structured replica of a house that imitates those located in our study area. Using the same data collection method with a drone loaded with a thermal camera, we corroborated the validity of our thermal data to some extent.

We now briefly summarize the analysis and results obtained herein. Based on the distance between houses, we conduct a hierarchical cluster analysis (single-linkage clustering) to group homeless persons' houses into clusters. Assuming that social interaction only works effectively within clusters of houses, we adopt cluster size (the number of houses in a cluster) as our agglomeration variable to express the magnitude of social interaction based on geographic proximity. Since the cluster size variable is time-invariant in our study period, we implement a random effects (RE) model. As expected, the baseline estimation result confirms that the larger the cluster size (the larger the social interaction network), the higher the living standard of the homeless persons in that cluster, as captured by house temperature. However, this result suffers from two sources of endogeneity of the cluster-size variable, one stemming from unobservable individual-specific characteristics and the other from unobservable location-specific characteristics.

---

<sup>6</sup>The exteriors of the houses of homeless persons, such as the walls or roofs, are often thin and it is possible for heat inside a house to leak; see Section 2 for a more detailed explanation.

The endogeneity originating from unobservable individual-specific characteristics—such as differences in ability, intellectual level, and physical handicaps—can be addressed by introducing individual fixed effects, which are impossible in our dataset, as the cluster-size variable is time-invariant. However, the direction of bias can be negative because homeless persons with unobservable low abilities may gather into larger clusters to seek greater support from interactions with other homeless persons (negative sorting). This expectation implies that the positive association between the cluster-size variable and the homeless person’s living standards should be strengthened (become more positive) if the individual unobserved characteristics were removed.

The other source of endogeneity due to unobservable location-specific characteristics can be addressed by instrumenting the cluster-size variable. As an instrumental variable for cluster size, we employ a dummy variable that equals one if a house is located on an inner curve of a meandering river and zero if it is located on an outer curve. Areas on an inner curve should be more suitable to build houses due to the presence of flatter land compared to locations on an outer curve, where the slope is usually steeper. Thus, larger clusters of houses are more likely present on inner rather than the outer curves.

Even after instrumenting the cluster-size variable by the inner/outer curve dummy variable, the significantly positive coefficient on the cluster-size variable remains unchanged, meaning that a larger cluster size leads to higher living standards for homeless persons in that cluster through the channel of a larger social interaction network. Although we cannot resolve the endogeneity caused by unobservable individual-specific characteristics, the significantly positive coefficient of the agglomeration variable after instrumenting suggests a positive effect for social interaction since the coefficient without resolving the unobservable individual-specific characteristics can have a downward bias, as addressed above.

The remainder of this paper is organized as follows. Section 2 describes the background of our study area and why we used a drone for data collection. Section 3 describes how we collected our data on which basis we conduct a cluster analysis to group observed houses into an appropriate number of clusters; we propose measures for house agglomeration (cluster size). Section 4 displays the results based on the baseline RE model; after addressing the two endogeneity issues caused by unobservable individual- and location-specific characteristics, we present the instrumental variable results to resolve the latter endogeneity issue. Sections 5 and 6 exhibit various robustness checks, which reveal that the results obtained in Section 4 remain unchanged. Section 7 raises some concerns about our thermal data and demonstrates the data’s validity by presenting the characteristics of the thermal data collected in

the replication experiment. Finally, Section 8 concludes the paper.

## 2 Background on the Homeless and Advantages of Utilizing a Drone for Data Collection

### 2.1 Benefits of Residential Agglomeration for Homeless Persons

A key factor in the positive impact of residential agglomeration is social interaction among homeless persons who live close together. Three types of benefits may arise for homeless persons living in a cluster from the perspective of social interaction: (i) gains from information diffusion, (ii) mutual aid, and (iii) mental well-being through mutual friendships.

Information sharing is important among homeless persons (Wolch et al., 1993; Yamakita, 2006). In our study area, information diffusion via social interaction is considered an essential benefit to homeless persons. The benefit from information diffusion for homeless persons is related to daily income and expenditures. One main income source for homeless persons in this area is collecting aluminum cans or used metal found in garbage disposal locations in non-homeless residential areas. Selling collected cans to scrap firms illegally is one way that homeless persons can earn money.<sup>78</sup> Individuals must have knowledge of which scrap firms conduct informal transactions. Without this information, individuals can neither sell collected cans nor exchange them for money because only a few scrap firms conduct illicit transactions with homeless persons. Such informal knowledge is only available through interaction with homeless friends; thus, information diffusion via interaction with other homeless persons is vital.

On the expenditure side, knowing which supermarkets sell inexpensive food at discounted prices or food shops let homeless persons have waste food is helpful. Since food scarcity is a major obstacle for the homeless (Division of Health & Welfare in Kawasaki City, 2019), shared knowledge about access to inexpensive food providers alleviates anxieties about food deficiency.

In terms of mutual aid, one of the most important benefits of living in a cluster is protection from violence from passersby or juvenile delinquents. Harassment and violence from non-homeless people

---

<sup>7</sup>In most administrative divisions in Japan, local ordinances forbid the collection or transportation of resources disposed in garbage collection areas, except by business firms entrusted by the local government. This is why activities of homeless persons such as collecting cans and selling them to scrap firms are deemed illegal in Japan.

<sup>8</sup>It is rare for homeless persons in Japan to beg for money or food from passersby (Okamoto, 2007). In the neighborhoods of our study area, approximately 70% earn money independently. On average, they earn approximately \$ 350–400 US per month. Among homeless earners, 82% obtain income by collecting and selling cans to illegal scrap firms and 11.5% work as daily construction workers (Division of Health & Welfare in Kawasaki City, 2019).

are ranked as the greatest anxieties for homeless people (Division of Health & Welfare in Kawasaki City, 2019; Sugita et al., 2010). Living near other homeless persons may keep them from being badly injured. In addition, in daily life, sharing food when a person cannot earn enough money is one example that highlights the necessity of mutual aid among homeless neighbors. Because income is obtained by collecting and selling cans and metal illicitly, the amount of money earned will change each day. An unreliable income may be relieved by mutual aid among homeless persons who live close together. Likewise, individuals can obtain hand-me-down electromechanical devices or useful goods from other homeless persons.

In terms of mental well-being, daily contact with other homeless persons in the same cluster may improve mental satisfaction. Loneliness is a major factor of mental illness, and even simple daily communication benefits homeless persons.

These social interaction factors may improve the quality of life for the homeless, so we expect that larger social networks (i.e., more homeless persons living close together) may raise living standards. To perceive the impact on homeless persons' material well-being provided by social interaction, we must obtain two types of information about the homeless persons in our study area: (i) interaction among homeless persons within the reach of their daily activity and (ii) their actual living standards. However, there is no straightforward way of extracting such information from homeless persons. In Section 2.2, we discuss why it is difficult to obtain this information and how we overcame or circumvented such obstacles.

## **2.2 Observing Interactions among Homeless Persons Based on Geographic Proximity**

Our case study can address the obstacles to obtaining information about interaction among homeless persons. The homeless persons in our study area settle in fixed locations by building cage-like houses in which they illegally occupy public land. Some unique features of the exteriors of these houses and sociodemographic characteristics enable us to approximate the house locations, with which we can obtain information about geographic proximity. We utilize the house-location information to group individuals into clusters based on the between-house distances. We implicitly assume that geographic proximity can be used as a proxy for social interactions,<sup>9</sup> and we use cluster size (the number of houses

---

<sup>9</sup>Bayer et al. (2008), Hellerstein et al. (2011), and Schmutte (2015) use geographic proximity as a proxy for social interaction. This paper follows this strand of identifying social interactions, and we assume that homeless persons in the same cluster interact with each other rather than with those in different clusters. Moreover, Section 3.3 considers the effect of geographic distance between any two persons within the same cluster.



in each cluster) as a proxy for social network size.

We start with an assumption that each house is occupied by one resident, so the number of houses can be viewed as indicating the number of homeless persons in the network. We defend this assumption by describing the sociodemographic characteristics of homeless persons in our study area. Unlike nomadic young homeless persons, whose temporary locations can be difficult to detect, some older homeless persons, mainly single males without families,<sup>10</sup> settle in stations, city parks, or riverbanks (Division of Health & Welfare in Kawasaki City, 2019). In 2018, 49.7% of homeless men in Kawasaki Ward (where our study area is located) were settled in cage-like houses that they had built on the banks of the Tama River (Division of Health & Welfare in Kawasaki City, 2019).<sup>11</sup> Many of the current homeless persons in Japan served as construction workers or were engaged in the manufacturing sector during the era of high economic growth, and such workers lost their jobs after the industrial structural shift at the end of Japan’s high economic growth period after WWII (Division of Health & Welfare in Kawasaki City, 2019; Iwata, 2004; Takano et al., 1999). These ex-construction workers may well have the ability to build simple-structure houses if they find a suitable and affordable location. The riverbank is evidently a suitable site to build such houses. Moreover, most of the homeless persons in Japan are older single men (Ito et al., 2014; Okamura et al., 2014), and this situation is consistent in our study area (Division of Health & Welfare in Kawasaki City, 2019).<sup>12</sup>

To obtain the location information of the cage-like houses, we captured aerial images with latitude–longitude and height information via drone and detected house-like objects appearing in the high-resolution aerial pictures. The typical exterior characteristics for the houses built by homeless persons in the study area enable us to detect what objects in the images are houses. The houses are usually rectangular or cuboid polygons with an edge length greater than 1.5 *m* when seen from above and covered by blue, green, or gray plastic sheets. We detected houses by considering the object height information from a set of polygons that satisfy the above features, i.e., we selected polygons whose heights exceed 1 *m*. After detecting houses, we calculate the distance between house centroids for each pair of houses. Based on this information, we grouped detected houses into clusters within which homeless persons were assumed to interact. As most of the homeless persons in this area are single

---

<sup>10</sup>The characteristic that homeless persons tend to be single males is also common in other countries. In European countries, the homeless are predominantly men, and most are unemployed and unmarried (Philippot et al., 2007). In the United States, the length of homelessness is longer for never-married men (Allgood and Warren Jr, 2003). Similarly, in Australia, men are more likely to sleep on the streets (Cobb-Clark et al., 2016).

<sup>11</sup>Sugita et al. (2010) find a similar settlement tendency for homeless persons in their field survey near the Tama River.

<sup>12</sup>According to the Division of Health & Welfare in Kawasaki City (2019), the average age of homeless persons in Kawasaki Ward was 62.3 years: 47.5% were in their sixties and 24.9% were older than 70 years in 2018.

males, it is reasonable to assume that each house is occupied by a single man. This assumption enables the conversion of house locations into individual locations.<sup>13</sup>

### 2.3 Observing the Living Standards of Homeless Persons

The obstacle to eliciting homeless persons' actual levels of living standards is a result of mental illness, alcoholism, and intellectual impairment among the homeless. As in many other countries,<sup>14</sup> there is a strong tendency for homeless persons in Japan to have mental disorders or cognitive impairment, such as hallucinations and delusions (Ito et al., 2014; Morikawa et al., 2011; Nishio et al., 2017; Okamura et al., 2014, 2015). Likewise, alcoholism is prevalent among homeless persons, and the morbidity rate of alcohol psychosis or alcohol-dependence syndrome is much higher than the Japanese average (Morikawa et al., 2011; Takano et al., 1999). In addition to the mental illness and alcoholism, there is a problematic prevalence of low IQ, cognitive disorders, and intellectual impairment among homeless persons (Nishio et al., 2017; Okamura et al., 2015).

These problems may induce severe difficulties in interviewing homeless persons because eliciting reliable information is extremely challenging. In a survey of mental illness among homeless persons in Tokyo conducted by Morikawa et al. (2011), the authors were unable to interview individuals who were drunk or experiencing hallucinations. The inaccessibility of these homeless persons made the authors conclude that the morbidity of mental illness among the homeless in their study area is underestimated.

Another limitation in interviewing homeless persons is noted by Salize et al. (2002). Even when homeless persons do not suffer from intellectual disability, mental illness, or substance abuse, the interviewers can only easily reach accessible groups of homeless persons such as users of shelters or people who come for free meals; this challenge can induce potential selection bias problems.

These problems would also emerge in our study area if we were to conduct a survey based on

---

<sup>13</sup>The possibility remains that some of the detected houses were vacant. To overcome this issue, we only considered those house polygons that show a variation in house temperature for the final sample of houses. As will be explained later, we consider house temperature a sign of human activity, so house polygons without temperature variations, which have a high possibility of having been abandoned, should be excluded from the sample.

<sup>14</sup>In Western Europe, the prevalence of mental disorders is high among the homeless (Philippot et al., 2007). In a field survey in the inner-city area of Mannheim, Germany, the prevalence of alcoholism or alcohol abuse was high (Salize et al., 2002). Moreover, Philippot et al. (2007) report that the majority of homeless people in Western European countries suffer from illegal drug abuse. Similarly, in the United States, a history of alcohol or illicit drug use increases the probability of becoming homeless (Early, 2005), and homelessness spells tend to be longer for persons with such problems (Allgood and Warren Jr, 2003). In addition, significantly lower IQ scores and a stronger prevalence of intellectual disability among the homeless population are observed in the United Kingdom (Oakes and Davies, 2008) and the Netherlands (Van Straaten et al., 2014). According to these findings, problems conducting interviews targeting homeless persons are common in many countries, given the similar tendencies regarding mental illness, substance abuse, and intellectual disorders.

questionnaires or interviews of homeless persons. The Division of Health & Welfare in Kawasaki City (2019) notes that homeless persons in our study area often suffer from alcohol or gambling addictions. Thus, instead of adopting an interview- or questionnaire-based approach, we collected house temperature data using an infrared thermal camera loaded on a drone to elicit information about living standards. This approach was based on the assumption that house temperature in the winter can be used as a proxy for the standard of living of residents in houses. The advantage of using a drone loaded with a thermal sensor is that it can collect thermal data by sensing various objects continuously and constantly from the sky.<sup>15</sup> Such uniformity in data collection can circumvent sample selection problems and unreliable information from homeless persons with intellectual and mental disorders.

Despite the usefulness of the combination of infrared thermography and drones, one may cast doubt on the validity of using surface temperature of a house as a proxy for the living standard of its resident. The following two questions about the validity may arise: (i) Does the night-time house temperature in winter express the level of resident living standards? (ii) If so, does the surface temperature of a house necessarily capture the inside temperature?

For the first question, we assume that the house temperature at night during the winter accurately represents the living standard of a homeless resident for the following reasons. As observed in Murata (2015), several homeless persons in our study area have electronic generators and electromechanical devices. Because using these electromechanical products generates heat, the house temperature of an individual who owns multiple electromechanical devices should be higher than that of a person who does not have such heat-producing devices. Moreover, winter is when homeless persons suffer the most from the cold (Division of Health & Welfare in Kawasaki City, 2019). They would want to avoid being cold if possible, and indeed, more well-off homeless persons can increase their warmth using heat-generation equipment. By contrast, poor homeless persons may not be able to stay warm, as they lack sufficient heat-generation products.<sup>16</sup>

Another important issue is whether residents are staying in their houses, but this may not be a major problem due to homeless persons' behavior. Usually, homeless persons earn money by collecting

---

<sup>15</sup>Akiyama et al. (2019) report the possibility of detecting vacant houses using drones. The presence of life activity producing waste heat was observed, and vacant houses showed no heat loss from house windows and walls. The authors emphasize that this observation is more valid during winter and at night. During winter, heat from solar radiation resolves faster during the day. Specular reflectance is also avoided at night, allowing the researchers to sense only the heat transfer from human activity.

<sup>16</sup>In summer, people prefer to cool down their house, so it would be unclear whether the houses of more well-off homeless persons show higher or lower temperatures; this ambiguity does not occur in winter.

used cans and selling them to illegal scrap firms, as already mentioned. In the morning, each Japanese household disposes of used cans at garbage sites set by local administrations. Homeless persons collect these cans in the morning, which means there is scant possibility they are at home during the daytime. Thus, it may not be appropriate to measure house temperature during the daytime, and we conjecture that the homeless are only consistently in residence in the evening. Thus, data collection at night is preferable, which is why we collected the thermal data at night.

Regarding the second question about external vs. internal heat, the outside surface temperature of a house roof should be an indicative of the inside temperature. Balaras and Argiriou (2002) note that thermal infrared images taken by thermography cameras are useful for noncontact detection of how energy leaks from a building's envelope. As an object's temperature correlates with the infrared radiation it emits, infrared inspection of building envelopes can detect heat losses from walls or roofs. We can measure inside temperature that leaks out through walls or roofs when they are thin. Indeed, the walls of homeless persons' houses tend to be very thin, and sometimes houses are simply constructed of frameworks covered by plastic sheets such that the houses are well ventilated (Murata, 2015).

Moreover, as discussed in Section 7, we conducted a thermal experiment in which we built an facsimile of a typical house from the study area. We measured the indoor temperature and sensed it using a thermal infrared camera attached to a drone. The obtained temperature data suggest that a higher drone temperature is associated with a higher indoor temperature. Hence, the house surface temperature recorded by drone is reasonably a good proxy for the inside temperature.

### **3 Data and the Empirical Model**

#### **3.1 Data Collected by Drone**

A flight campaign was conducted using a Matrice 210 drone with a thermal Zenmuse-XT2 camera (DJI, Shenzhen, China). The altitude of the drone was 140 *m* above the ground, and aerial images were continuously taken with the camera facing a nadir along the river edges. The aerial survey obtained thermal information and location data of houses of homeless persons on the Kanagawa Prefecture side of the Tama River. Flight permission was obtained following aviation laws, and extreme care was taken with the flight altitude and geographic position of the survey due to the presence of the nearby Haneda Airport. Despite the care taken when flying drones along the Tama River, limitations arose in the data collection. First, we were unable to collect data from houses underneath bridges to prevent

possible accidents caused by crashing into the bridge. We will return to this point in Section 6.7 when we check whether the results change if we exclude house observations near bridges from our sample.

The study area is known for homeless persons illegally occupying the land in cage-like, rectangular-shaped houses that are usually covered with blue, green, or gray plastic sheets.<sup>17</sup> Since these house features are most common in the target area, we first detected house locations by viewing drone-collected image data from the daytime on February 17, 2019. We extracted house-like objects that have the following features: (i) a rectangular or box shape, (ii) covered with blue, green, or gray plastic sheets, and (iii) sufficient size for a person to reside (e.g., sides longer than approximately 1.5  $m$  and height greater than approximately 1  $m$ ). We identified 63 house-like objects that satisfy these conditions. Figure 1a displays a sample of the detected house polygons highlighted by light blue lines.

[Figure 1 around here]

Figure 2a shows the entire study area, with each house given a unique house ID from 1 to 63.

[Figure 2 around here]

Each point in Figure 2a represents the centroid of a house, and the blue band running from the southeast to the northwest is the Tama River. Since houses are aligned in a narrow space along the river that is nearly linear, each house is assigned a unique ID whose numbering starts from the house located in the southeast end (house 1) and ends at the northwest end (house 63). The ID number is based on the number of houses up from house 1 along the river and the distance from house 1 to 63 along the river is about 7.1  $km$ .

To collect the thermal temperature data from each house,<sup>18</sup> we flew our drone three times in winter 2019. Our drone flights were conducted at 18:48–21:13 on February 17, 19:15–22:07 on March 14, and at 19:10–21:24 on March 15. Our night-time collection of temperature data is appropriate because of the disturbance of solar radiation during daytime. Heating material during the day causes limitations in observing the direct source of heat waste, and the specular reflectance of solar radiation causes observation errors, which is avoided in night-time data collection.<sup>19</sup>

---

<sup>17</sup>Figure OA1 in the online appendix shows typical houses of homeless individuals in this area.

<sup>18</sup>The thermal temperature of an object can be calculated from the emitted electromagnetic energy based on the Stefan–Boltzmann law. The Zenmuse-XT2 (DJI, Shenzhen, China) thermal infrared camera observes the spectral range of 7.5–13.5 $\mu m$ . The system senses thermal infrared waves and converts electronic signals into absolute temperature information.

<sup>19</sup>According to Balaras and Argiriou (2002), infrared measurements should be performed at night or during cloudy days without high wind speeds. Drone flights using Zenmuse-XT2 cannot be performed on windy or rainy days, and our house temperature data (infrared thermal image data) were collected by a drone with a thermal sensor at night, meaning that the temperature data were collected under appropriate conditions.

We match the house-location data and house-temperature data by assuming that during our study period (February 17–March 15) there was no relocation of houses detected in the daytime images taken on February 17.<sup>20</sup> Figure 1b displays a sample of the thermal images matched with house polygons.<sup>21</sup> After separating out the part covered by edges and leaves to avoid capturing the temperature of vegetation covering rooftops, we calculate the average of temperature over the house polygon for each house and assign this average house temperature to each house location.<sup>22</sup> Figure 1c illustrates the average house temperature over each polygon, corresponding to the house polygons in Figures 1a and 1b. Hereafter, we call this average temperature over each house polygon the house temperature for each house.

Notably, even though we have 63 house-location observations from the daytime flight, some of these 63 houses lack nighttime temperature values for two reasons, the first of which is technical limitations. Some houses have no temperature values due to the daytime visual images having higher resolution levels than the nighttime thermal images. For observations with roofs covered by tiny leaves or thin edges, we know from the higher-resolution daytime aerial images that houses exist there even when their roofs are covered by vegetation. In the night-time thermal images characterized by lower resolution, we cannot distinguish roof parts covered by tiny leaves or edges from those not covered by such vegetation. Essentially, mixing of roof parts covered by vegetation and those uncovered occurs in the thermal images. This issue prevented us from calculating the average house temperature over the polygon by removing the part covered by vegetation. Hence, houses 30, 48, 49, and 53–55 have missing house temperature values for all dates.

The second reason for missing nighttime house temperature values is simply human error. The nighttime flights were less visible than the daytime flights, so the former have more difficulty distinguishing objects than the latter. Moreover, it is challenging to obtain thermal images of exact points at night; thus, some houses have missing temperature values. Houses 1, 12–17, 47, and 50–52 lack house temperature data for February 17 for this reason, whereas there are no missing house temperature values for March 14 or 15. Due to these two sources of missing values, we obtained 46 observations for February 17, 57 observations for the other two dates, and thus 160 records in total.

---

<sup>20</sup>It is unlikely that house relocation would occur in such a short time period (approximately one month).

<sup>21</sup>The collected aerial images are in radiometric JPEG (R-JPEG) format. The temperature information is extracted from the R-JPEG data using the FLIR Tools software ver. 6.4 (FLIR, Wilsonville, U.S.). The “box tool” is used to cover the area of the house polygons, and the average and maximum temperature values for each house polygon are extracted.

<sup>22</sup>It is natural for a house polygon to have different temperature values at different points over the polygon. To obtain a representative variable that expresses each house temperature, we calculated the average temperature over the polygon area for each house in our baseline model.

### 3.2 Cluster Analysis

As addressed in Section 1, this paper’s objective is to determine whether residing in clusters benefits homeless persons and the extent of this benefit. We first detected the clusters of homeless persons’ houses that appear in Figure 2a using hierarchical cluster analysis. We adopted single-linkage clustering because of its chaining property, which means that a cluster created in single-linkage clustering has the shape of a line (chain). As the houses of homeless persons are located in a narrow area along the river, they can be viewed as aligned in this manner. Thus, single-linkage clustering, which generates chain-like clusters, should be appropriate. In single-linkage clustering, the between-cluster distance (linkage function between two clusters,  $C_1$  and  $C_2$ ) is defined as

$$d_{single}(C_1, C_2) = \min_{i \in C_1, j \in C_2} d_{ij}, \quad (1)$$

where the distance between houses  $i$  and  $j$  is denoted as  $d_{ij}$ . In single-linkage clustering, the linkage score, or between-cluster distance, in (1) is the distance between the closest pair of houses where one belongs to cluster  $C_1$  and the other belongs to cluster  $C_2$ , which has no common elements (houses) with  $C_1$ . Starting from singleton clusters, we repeat the assignment to merge pairs of clusters with the shortest between-cluster distance (1), and the process ends when all houses are included in one identical cluster.

The distance between houses,  $d_{ij}$ , expresses how far homeless person  $i$  must travel to reach another homeless person  $j$ . As shown in Figure 2a, the river is meandering. Therefore, it is inadequate to calculate the direct distance between two houses because homeless persons do not walk over the river. Then, for  $i < j$ , where  $i$  and  $j$  indicate house IDs from 1 to 63, we define  $d_{ij}$  as

$$d_{ij} = \sum_{k=i}^{j-1} d_{k,k+1}, \quad (2)$$

which is obtained by summing the direct length between adjacent house centroids over house  $i$  through house  $j$  on the line connecting house centroids from house 1 to house 63.

Based on the dissimilarity matrix whose  $(i, j)$ -th entry is  $d_{ij}$ , we run single-linkage clustering to obtain the dendrogram in Figure 3a.

[Figure 3 around here]

The number of clusters differs depending on the height at which the dendrogram is horizontally cut.

The next step is to determine the optimal number of clusters, accompanied by the determination of the grouping of the houses. To do so, we calculate the Calinski-Harabasz index ( $CH$ -index) under the possible numbers of clusters to find the number of clusters that returns the maximum  $CH$ -score. The  $CH$ -index is the ratio of the between-cluster variation (which measures how spread out the clusters are from each other) to the within-cluster variation (an inverse measure of how tightly the clusters are grouped).<sup>23</sup> With this definition, the number of clusters that gives the maximum  $CH$ -score should be the optimal number of clusters. Figure 3b shows the  $CH$ -scores under different numbers of clusters for  $K = 2, \dots, 30$ .<sup>24</sup> From Figure 3b, the  $CH$ -index calculated with  $K = 4$  achieves the local maximum but not the global maximum. The  $CH$ -score generally increases for  $K \geq 10$  in the figure. In such a case, the clusters are not considered well-separated, because the  $CH$ -index does not have a global maximum. However, if an optimal number of clusters exists, the likeliest number is  $K = 4$ , according to Calinski and Harabasz (1974). Thus, we adopt  $K = 4$  as our optimal number of clusters. From the dendrogram shown in Figure 3a, when the number of clusters is 4, the houses are grouped as follows: cluster 1 = [1–17], cluster 2 = [18–46], cluster 3 = [47–52], and cluster 4 = [53–63], where the numbers in the brackets indicate the house IDs.<sup>25</sup> Figure 2b shows the four clusters of houses. Hereafter, the clusters referred to in our analysis are the four clusters depicted in Figure 2b.

### 3.3 Measures of House Agglomeration

We consider variables that measure the extent of agglomeration (i.e., cluster size) of homeless persons. As mentioned in Section 2, homeless persons may improve their living standards by helping each other, so the larger the number of homeless persons residing in a neighborhood, the more the person’s life will improve. The number of houses in the same cluster or the cluster size, captures this aspect. As an immediate measure of cluster size, we adopt  $N(i)_{-i} \equiv N(i) - 1$ , where  $N(i)$  is the number of houses in cluster  $C(i)$ , which house  $i$  belongs to.

Although  $N(i)_{-i}$  is a direct variable, it does not consider the distance between houses within a cluster, which may matter because people will interact more with those located closer than those who are farther away. Thus, we modify  $N(i)_{-i}$  to take into aspect by discounting the number of

<sup>23</sup>For the  $CH$ -index used in this paper, see Appendix A.1.

<sup>24</sup>The  $CH$ -scores can be obtained for  $K = 2, \dots, 63$ , although Figure 3b shows only  $K = 2, \dots, 30$ .

<sup>25</sup>One may think that, in our case, the houses are positioned in one-dimensional space. With this interpretation of the space of our study area, some may prefer an analysis based on segmentation of the interval rather than cluster analysis. Therefore, we also conducted a segmentation analysis to identify the grouping of the houses that minimizes the sum of the within-group sum of squared deviation from the group mean at a given number of groups,  $\hat{K}$ , following Fisher (1958). The results based on segmentation support the same classification of houses as that obtained via single-linkage clustering. For details, see Appendix A.2.



houses by distance to other houses in the same cluster. The simplest modification of  $N(i)_{-i}$  is the distance-discounted number of houses in  $C(i)$  except house  $i$ :

$$DN_{-i}(i) \equiv \sum_{j \in C(i) \setminus \{i\}} e^{-d_{ij}} = \sum_{j \in C(i)} e^{-d_{ij}} - 1 \equiv DN(i) - 1, \quad (3)$$

where  $DN(i)$  is the distance-discounted total number of houses in cluster  $C(i)$ .<sup>26</sup>

### 3.4 Empirical Model

Our hypothesis is that homeless persons residing in larger clusters are better off, which is translated into the hypothesis that the temperature of a house located in a larger cluster is higher. Note here that  $N(i)_{-i}$  and  $DN(i)_{-i}$  are time-invariant variables (i.e., they take the same values across all three dates, as they are based on only the house locations). Then, the estimation model is forced to be an RE model:

$$\text{HouseTemperature}_{ictd} = \beta_0 + \beta_1 \text{Agglomeration}_{ic} + \beta_2 \text{OutsideTemperature}_{itd} + \beta_3 X_i + \theta_d + \nu_i + \epsilon_{ictd}, \quad (4)$$

where  $\text{HouseTemperature}_{ictd}$  is the temperature of house  $i$  in cluster  $c$  at time  $t$  (recording time of the temperature of house  $i$ ) on date  $d$ .<sup>27</sup>  $\theta_d$  is the date fixed effects,  $\nu_i$  is house random effects assumed to satisfy  $E(\nu_i) = 0$  and is uncorrelated with other explanatory variables of house  $i$ ,<sup>28</sup> and  $\epsilon_{ictd}$  is a stochastic disturbance.  $\text{Agglomeration}_{ic}$  is either  $N(i)_{-i}$  or  $DN(i)_{-i}$  proposed in Section 3.3.

$\text{OutsideTemperature}_{itd}$  is the outside temperature in the neighborhood of house  $i$  at time  $t$  on date  $d$ . As mentioned in Section 3.1, the house temperature data collection time for each house was at the minute level. Ideally, the outside temperature data would be collected at exactly the same location of the houses at the same time, but this was not possible due to the outside temperature data availability. The data we have is outside temperature data recorded every 10 min at two sites, Haneda and Fuchu, the automated meteorological data acquisition system (AMeDAS) stations closest

<sup>26</sup> $d_{ij}$  in (3) is measured in kilometers. Then, for example, in cluster 1, the magnitude of  $e^{-d_{ij}}$  for house 1, the most peripheral house in the cluster, ranges from  $e^{-d_{1,2}} \approx 0.797$  to  $e^{-d_{1,17}} \approx 0.438$ . Additionally, for house 9, the most central location in the same cluster, it ranges from  $e^{-d_{9,8}} \approx 0.974$  to  $e^{-d_{9,1}} \approx 0.596$ .

<sup>27</sup>Some may wonder why time fixed effects ( $\mu_t$ ) do not appear in the estimation model (4). As will be described in the explanation of the variable  $\text{OutsideTemperature}_{itd}$ , we have access to outside temperature data recorded every 10 min, but it is impossible to include time fixed effects at 10 min intervals in our estimation model due to the small sample size (63 houses and 160 observations in total). Thus, we prefer to make use of outside temperature data at 10-min intervals instead of time fixed effects with time intervals longer than 10 min.

<sup>28</sup>This assumption of the RE model is not supported in some of the specifications, and we think that  $\nu_i$  is correlated with  $\text{Agglomeration}_{ic}$ . This endogeneity problem is discussed in Section 4.2.

to our study area. The AMeDAS is a collection of automatic weather stations operated by the Japan Meteorological Agency for automatic observation of precipitation, wind direction/speed, temperature, and sunshine duration to support real-time monitoring of weather conditions.<sup>29</sup>

To fit temperature data recorded by the AMeDAS to our dataset, we construct the outside temperature data via the following procedure. First, from the set of reported times in the AMeDAS data, we choose the closest time to time  $t$ , which is the time at which house  $i$ 's temperature was collected by the drone. Then, we calculate the distance-weighted value of the outside temperature at the time chosen above based on the direct distance from house  $i$  to the two AMeDAS stations:

$$\begin{aligned} & \text{OutsideTemperature}_{itd} \\ &= \frac{\text{OutsideTemperature}_{\text{Haneda},td} * \text{Distance}(\text{House}_i, \text{Fuchu})}{\text{Distance}(\text{House}_i, \text{Fuchu}) + \text{Distance}(\text{House}_i, \text{Haneda})} \\ &+ \frac{\text{OutsideTemperature}_{\text{Fuchu},td} * \text{Distance}(\text{House}_i, \text{Haneda})}{\text{Distance}(\text{House}_i, \text{Fuchu}) + \text{Distance}(\text{House}_i, \text{Haneda})}. \end{aligned}$$

$X_i$  is a set of time-invariant variables of house  $i$  other than  $\text{Agglomeration}_{ic}$  to control for natural and geographic aspects and the amenity effect.<sup>30</sup> We include a forest-coverage variable, a grass-coverage variable, the distance to the river shore, and the distance to the nearest freely available toilet/tap in the riverside area.<sup>31</sup> Figure 4a is a map of a toilet/tap location layer superimposed on the house-location layer.

[Figure 4 around here]

A sufficiently large number of toilets and taps are located in the riverside area, so homeless persons can have frequent and daily access. Hence, we expect that the access to toilets and taps improves the living standards of homeless persons in this area.

For the forest- and grass-coverage variables, we create a 5- $m$  buffer from the house edges and calculate the percentage of land covered by either trees or grass.<sup>32</sup> The variable distance to the river shore is the shortest distance between a house edge and the river shore. These three variables are related to geographic and natural characteristics that may directly affect the house temperature; land areas covered by grass or trees may be warmer than barren areas in the winter. Moreover, distance

<sup>29</sup>See Figure OA3 in the online appendix for the positional relation of the two AMeDAS stations, Fuchu AMeDAS station and Haneda AMeDAS station, and our study area.

<sup>30</sup>Data sources are listed in Table OA1 in the online appendix.

<sup>31</sup>Figure OA2 in the online appendix is a picture of a toilet and a tap in the riverside area. Tap water is available at the site where the toilet is located.

<sup>32</sup>For the grass-coverage variable, we assume that grass covers the land hidden by trees in the aerial images.

to the river shore may affect house temperature because, due to the specific heat of water, the water temperature may be higher than the land temperature on winter evenings.

The distance to the nearest toilet/tap plays a different role in impacting the house temperature. Recall that house temperature is a proxy for the living standards of the homeless person residing in the house, and our objective is to see how well-off the individual is. Distance to the nearest toilet/tap is considered to affect the living standards of homeless persons via a channel of improved access to the amenity, in contrast with variables such as outside temperature, vegetation coverage, and distance to the river shore, which directly affect house temperatures. We expect that better access to the sanitary amenity improves a homeless persons' living standards, which leads to a higher house temperature.

### 3.5 Summary Statistics

Table 1 shows the summary statistics of the variables used in the estimation, including those used in the baseline model and those used in the robustness checks that appear in Sections 5 and 6.

[Table 1 around here]

One thing to notice about the statistics in Table 1 is the house temperature values. The house temperature variable shows values lower than the outside temperature, and they sometimes take negative values. This seemingly unnatural tendency of house temperature is in fact natural, because the temperature of an artificial building measured from the outside is often lower than that in the vegetation area or the outside temperature, differing depending on materials (Michell and Biggs, 1979).

The fact that the artificial materials show lower temperatures than natural objects does not hinder our analysis, because we are measuring temperatures radiating from the inside to the outside of houses and conducting a comparison between artificial objects (houses of homeless persons), not between artificial and natural objects. Moreover, as described in Section 2, due to the lightness of structures of the houses, which have thin walls and roofs covered by plastic sheets to maintain sufficient permeability, we conjecture that it is possible to measure from an outside position the heat radiating from inside.

In addition to the above discussion, we show the validity of thermal data we use in the main analysis in Section 7.2, exhibiting the summary statistics of the temperature data collected in a thermal experiment. In the experiment, we both collect thermal data of the temperature inside a replica house and that recorded in drone flights. Comparison between two temperature datasets suggests that even when a temperature recorded by a drone is low, the inside temperature is much higher than the drone

temperatures. Specifically, the indoor temperature is sufficiently high for a person to reside there, even when the temperature sensed by a thermal camera carried by the drone is low.

Before proceeding to the estimation results, we briefly consider the relationship between house temperature and the cluster size for each date in Figure 5.

[Figure 5 around here]

In Figure 5a, the horizontal axis is the number of houses in a cluster  $N(i)_{-i}$ , and the vertical axis is the net house temperature, defined as the house temperature minus the outside temperature. As explained in Section 3.1, some houses have missing temperature values, so only three clusters appear in the panel for February 17. Panels of the other dates display four clusters; the largest cluster, with  $N(i) = 29$ , is houses 18–46 (cluster 2 in Figure 2b), the next largest, with  $N(i) = 17$ , is houses 53–63 (cluster 1), the third largest, with  $N(i) = 11$ , is houses 53–63 (cluster 4), and the smallest, with  $N(i) = 6$ , is houses 47–52 (cluster 3). In all panels in Figure 5a, the cluster size and house temperature show a positive relationship, indicating that belonging to a larger cluster is associated with higher living standards. Taking  $DN(i)_{-i}$  as the cluster-size variable in Figure 5b, an analogous tendency can be found (i.e., house temperatures in a larger cluster measured by  $DN(i)_{-i}$  tend to be higher).

## 4 Estimation Results

### 4.1 Baseline Results

Because we aimed to test whether there is a positive effect on the living standards of homeless persons from residing in a larger cluster, we expected a positive sign for  $\beta_1$  in (4). Under the assumption that geographic proximity (in our case, belonging to the same cluster) is a proxy for social interactions,  $\beta_1 > 0$  can be interpreted as the existence of benefits from social interactions within a cluster.

Table 2 shows the results for the baseline model.

[Table 2 around here]

Columns (1) and (2) show the results of the pooled OLS (POLS) and RE models with  $N(i)_{-i}$  as the agglomeration variable.<sup>33</sup> Columns (4) and (5) are the corresponding results with  $DN(i)_{-i}$ . As

---

<sup>33</sup>We simply clustered the standard errors by houses, not by clusters because the wild cluster bootstrap for few clusters (we only have four clusters) is considered inapplicable in our situation, according to Canay et al. (2021). First, for the wild

expected, the coefficients of the agglomeration variables ( $N(i)_{-i}$  in column (2) and  $DN(i)_{-i}$  in column (4)) are significantly positive at the 5% level. When the cluster size is larger, each house has a higher temperature, indicating that residents with a larger within-cluster network may be better off.

The finding that homeless persons located in larger clusters tend to experience higher living standards does not result from the logic used in Culhane (2010), Corinth and Lucas (2018), and Lee and Price-Spratlen (2004), which sheds light on the gravitation of homeless individuals to services offered to them. In their research on homeless agglomeration, homeless persons in areas with homeless concentration benefit by agglomeration of services that target them, such as shelters, free meals, and soup kitchens. However, this mechanism does not apply to our case, because there are no facilities that offer services to homeless persons in the study area. Moreover, our interview with the Division of the Medical Welfare Services of Kawasaki City revealed that there were only three free meal services offered there per month. Rather than the logic proposed in the literature, our paper focuses on the aspects of social networks through channels of information diffusion and mutual aid that stem from interaction with other homeless persons living nearby.

One may also have concerns regarding the positive relationship between the house temperature and cluster size from a viewpoint of thermal radiation from adjacent houses. In other words, a house temperature may be high because heat radiating from other houses raises its temperature, which is more likely in a larger cluster. However, our thermal experiment reveals that the possibility of such a situation is low. As we see in Section 7, thermal radiation from a replica house is limited within only a geographically narrow range, and it is unlikely that heat radiating from a house affects the temperatures of houses nearby.

Next, we look at the coefficients of the other variables. The variable outside temperature is highly positively correlated with house temperature in both models, which is a natural result. Regarding distance to toilets and taps, its significantly negative coefficient can be interpreted as a sign that better access to an amenity improves a homeless persons' living standards. This result reflects the need for water for personal hygiene and clothes washing (Division of Health & Welfare in Kawasaki City, 2019), as well as for drinking clean water.<sup>34</sup> The finding that access to amenities such as a toilet and clean water is beneficial for the residents coincides with observations in slums in developing countries.

---

cluster bootstrap to work properly, relative sizes of clusters should not differ dramatically. This assumption, however, may not be satisfied in our case since we exploit the variation of sizes of clusters. The second assumption for the wild cluster bootstrap is that  $N(i)_{-i}$  should vary within the same cluster, which is not obviously satisfied in our case as the cluster size variable is identical within the same cluster.

<sup>34</sup>In Japan, tap water is good for drinking, so better access to taps means not only better access to water for washing but also for drinking.

Brueckner (2013) finds that residents in slum-like dwellings in Indonesia appreciate access to toilets and water sources. Similarly, having piped water connections to houses, toilets, and bathrooms is highly valued in slums in India (Takeuchi et al., 2008). In Lall et al. (2008), the authors find that households in squatter settlements in India derive benefits from neighborhood amenities and the quality of the dwellings, especially from a connection to the sewer. Moreover, Feler and Henderson (2011) note that, because water is essential, withdrawing water connections to a slum reduces growth rates of its population in Brazilian localities. It is natural to find the commonality between the residents in slums and the homeless persons in our case, because homeless persons in the study area occupy public lands and build houses illegally, similarly to urban squatters.

In addition, the significance of the positive relationship of better access to an amenity and homeless persons' living standards can be interpreted as being due to their not paying rent. By examining U.S. national data, Corinth and Lucas (2018) report that homeless persons are attracted to a mild climate, another important amenity. They ascribed the larger population of the homeless people in places with warm climates to the fact that climate is not directly reflected in the cost of living for homeless persons, who do not pay rent or mortgages. Analogous logic can be applied in our context. As better access to toilets and water is not reflected in rent, homeless persons living close to toilets/taps can benefit from better access to sanitation amenities without paying pecuniary costs, which leads to those having toilets/taps in their neighborhood being better off.

In terms of the vegetation coverage variables, forest coverage is positively correlated with house temperature. When surrounded by vegetation, especially trees, the house temperature is stabilized. Such vegetation may keep houses warmer in the winter and cooler in the summer. There may be another explanation for the vegetation-coverage variable. For homeless persons, being hidden from society at large is important. The denser the forest surrounding a house is, the less likely it is to be seen by non-homeless passersby, who sometimes harm homeless individuals through violence. The significantly positive sign of forest coverage and the significantly negative sign of distance to the river shore may reflect this advantage. As indicated by the significantly negative coefficient of distance to the river shore, house temperature is positively associated with river shore proximity, as expected. This may be due to the higher specific heat capacity of water than that of land.

## 4.2 Endogeneity Concerns

In Section 4.1, we confirmed that house temperature, a proxy for how well-off each homeless person is, is positively associated with cluster size. However, we believe there are two sources of endogeneity related to the cluster-size variable: unobservable individual-specific characteristics and unobservable location-specific characteristics.<sup>35</sup> In terms of the endogeneity due to unobservable individual-specific characteristics, we expect that the coefficient of the cluster-size variable suffers from downward bias. Homeless persons who are less able or more disadvantaged may prefer to reside in a larger cluster to seek greater support from other homeless persons. Those who do not have an ability to build quality houses due to physical disadvantages may want surrounding homeless persons to assist them. Those who cannot consistently earn enough money may want to stabilize their lives by sharing food or daily necessities with others.

In contrast, those with sufficiently high abilities do not need to rely on others and may prefer to live in isolation. Instead of seeking greater mutual support in a larger cluster, such able homeless individuals may want to live in a smaller cluster to avoid competition for cans or metal, which are limited income sources. Several garbage sites are evenly distributed near the study area, and various sites must be visited to collect a lot of cans. If there are many competitors in the neighborhood (i.e., many homeless persons in the same cluster), one can collect only a small amount of cans, which leads to lower earnings. A homeless person who can manage to live on their own may prefer to live in a smaller cluster to circumvent this impact on their earnings. In short, homeless persons unobservably less able may sort into larger clusters, while those with unobservable high abilities may sort into

---

<sup>35</sup>In assessing the agglomeration effect (measured by the population density in a city) on wages, two sources of endogeneity are recognized (Combes et al., 2010, 2011; Moretti, 2004). The first is unobservable worker-specific characteristics such as ability, which may cause an upward bias of the estimated coefficient of the density variable due to workers' positive sorting to larger (denser) cities, i.e., unobservably more competent workers sort into larger (denser) cities. With an access to individual panel data, it is recommended to eliminate individual fixed effects to resolve the endogenous quality of labor bias (Combes et al., 2010, 2011). The second source of endogeneity is unobservable city-specific characteristics. Cities with unobservably better amenities may attract workers, which raises population density in those cities. Employing instruments for the density variable is encouraged to resolve the endogenous quantity of labor bias (Combes et al., 2010, 2011).

smaller clusters.<sup>3637</sup>

Such endogeneity caused by unobserved individual characteristics should ideally be addressed by introducing individual fixed effects into the estimation model. Unfortunately, this option is not possible in our dataset, as our featured variable, cluster size, is time invariant in the study period. Nevertheless, if the estimated coefficient of cluster size is positive, then its real impact on house temperature should also be positive, because, following the above discussion of negative sorting into larger clusters, the naively estimated coefficient is considered to have a downward bias (the positive impact of cluster size may be underestimated).

Regarding the second source of endogeneity coming from unobservable location-specific characteristics (an unobservably beneficial location may attract more homeless persons) is addressed using an instrumental variable. An appropriate instrumental variable should affect the living standards of a homeless person only through the channel of house distribution. One possibility is a variable that expresses only the suitability for house construction in a particular area on the riverbank, as it is more likely that a larger cluster of houses is generated in areas suitable for building houses. A variable that indicates whether an area is located on the inner curve or outer curve can be used as an instrumental variable to capture this aspect.

To begin, we inspect house distributions on both sides (the Kanagawa and Tokyo sides) of the Tama River in 2020, as shown in Figure 4c.<sup>38</sup> From a casual observation, we find a tendency for there

---

<sup>36</sup>We do not deny completely the possibility that the cluster-size variable suffers from an upward bias (i.e., that more able homeless persons may choose to live in larger clusters). However, as is discussed in the main text, the income sources in the geographic scope they can reach, such as disposed cans and metals, are limited. Such income sources do not increase even when homeless persons agglomerate in larger clusters, because their knowledge exchange itself does not expand the pie of their income source (i.e., the number of cans and metals does not increase). The almost sole merit in terms of knowledge spillover by homeless persons' agglomeration comes from the access to information about which scrap firms informally transact with them. It is reasonable to consider that more competent homeless persons, who already know a lot about the area, may not need more homeless persons nearby, given their advantage from circumventing the homeless rivals who take the income sources available in the area. By contrast, less able homeless persons who have limited knowledge about their residential area are more urged by access to information about the scrap firms that make illicit transactions with them. Thus, the negative-sorting story seems to be more reasonable than the positive-sorting story, although the possibility of the latter is not perfectly eliminated.

<sup>37</sup>Unobservable heterogeneity among homeless persons does not largely come from demographic differences such as sex, age, and marital status, as most of the homeless persons in our study area are single older males. Thus, we focus on heterogeneity of ability and how disadvantaged a homeless person is as unobservable characteristics.

<sup>38</sup>Although we collected house distribution data in 2020, these data are not suitable for our formal analysis, as the house distribution is unstable and changed considerably in a short period in the winter of 2020. In October 2019, a large typhoon, named Typhoon 19, hit the study area, and most of the houses were washed away. This was broadcasted as a rare event that had not happened in the past 50 years (<https://www.sankei.com/article/20191013-DHD6RFIVIBNCZDIY4BPXT25SXY/> in Japanese, accessed at January 21, 2023). After a few months, we collected aerial images of houses built in January 2020, as depicted in Figure 4c. When collecting the house temperature data in February 2020, however, the house distribution appears to have changed further, possibly because this area was still in recovery. Moreover, due to leaves and edges carried away by the flood and piled up near houses, we were unable to construct vegetation variables. The data in the winter of 2020 is only employed for a casual observation. This is why we did not exploit the data in 2020.



to be almost no houses on the right-opposite side of the shore along which a house cluster is generated. In addition, more houses are located along inner curves than along outer curves. Usually, the two shores of a river can be approximated as a pair of nearly parallel lines, implying that the right-opposite side of an inner curve is an outer curve, and vice versa. On the basis of this observation, it can be conjectured that there are more houses located on inner curves than on outer curves. The tendency that riverside areas located on the inner curve accommodate more houses than those located on an outer curve may be due to the flatness of the land on inner curves compared to that on outer curves. Usually, inner curves are flatter because of sedimentation. By contrast, outer curves are steeper and narrower because of erosion. Thus, areas located on inner curves are often more suitable for building houses, entailing larger clusters of houses there.

Although it is impossible to prove that the inner/outer curve variable affects house temperature through only the cluster size channel, we address the concern about the violation of the exogeneity condition. The inner/outer curve variable may be correlated with house–river shore distance. As the area of inner curves tends to be flat and roomy, houses can be built farther inland. Therefore, houses being located on an inner curve is correlated with the distance from the houses to the river shore. However, this characteristic may not be likely in the case of our study area. In the riverbank area of the Tama River, even on inner curves, only the areas very close to the river shore are available for homeless persons. The inland area on the inner curve is used as playgrounds for non-homeless citizens, so whether a house is located on an inner or outer curve is not significantly correlated with distance between the shore and the house.

Another concern with the exogeneity of the instrument comes from whether there is a difference in flooding likelihood depending on whether houses are located on an inner or outer curve. If such a difference exists, homeless persons located on outer curves may be more heavily affected by natural disasters (note that the river flow is faster on outer curves). However, according to Murata (2015), the houses of homeless persons are built in areas that are usually not flooded and little affected by rising water levels. Thus, there may be no crucial difference between houses on inner and outer curves.

To construct the instrumental variable of inner/outer curves, we take the following four steps.<sup>39</sup> In the first step, we locate points every 1 *m* along the river shore in our study area.<sup>40</sup> In the second step,

---

<sup>39</sup>An illustrative image of constructing the instrumental variable is depicted in Figure OA4 in the online appendix.

<sup>40</sup>Instead of the line data of the river shore provided by the National Land Numerical Information Download Service, we use data that we constructed by delineating a boundary between the water area and the land area based on the aerial photographs provided by the Geospatial Information Authority of Japan (GIAJ). This is because the GIAJ line data are more convenient due to the smoothness of the shorelines

we draw straight lines connecting some of the points generated in the first step. In doing so, we admit that the newly drawn straight lines can depart from the actual river shore by 100 *m*.<sup>41</sup> In the third step, we identify whether the points generated in the first step are located on an inner or an outer curve: (i) if the straight line connecting two points drawn in the second step runs through land area, the points between these two points (two ends of the straight line) are located on an inner curve, and (ii) if the straight line connecting two points generated in the first step runs through water, the points are on an outer curve. In the fourth step, we find the nearest point among those generated in the first step for each house and assign the nearest point’s characteristic identified in the third step (i.e., whether the point is located in an inner curve or an outer curve) to each house. Finally, we obtain a dummy variable equal to 1 if a house is located on an inner curve and equal to 0 if it is located on an outer curve as the instrumental variable to implement the cluster size.

Columns (3) and (6) in Table 2 exhibit the REIV results for specifications based on the choice of  $N(i)_{-i}$  and  $DN(i)_{-i}$ , respectively. In the first-stage estimation, the instrumental variable shows sufficient significance, with the expected sign in all specifications (the sufficiently large F-statistic for the weak instrument), which supports the relevance of the instrumental variable. In the second-stage estimation, the coefficients of the cluster-size variables,  $N(i)_{-i}$  and  $DN(i)_{-i}$ , exhibit strong positive significance with respect to cluster size, indicating that living among more homeless persons may improve living standards. Moreover, the coefficient value in the  $N(i)_{-i}$  specification can be interpreted in a way that an additional house in the same cluster increases 0.195°C of house roof temperature recorded by a drone (Column (3)). In the same vein, an additional increase of a distance-discounted house raises a house roof temperature by 0.268°C (Column (6)).

Next, to consider the direction of the bias, we compare the RE and REIV results. By comparing the coefficients of cluster-size variables in columns (2) and (3) for the  $N(i)_{-i}$  specification and in columns (5) and (6) for the  $DN(i)_{-i}$  specification, we see that the uninstrumented estimates are negatively biased in both specifications. In fact, this downward bias of the instrumented result is unexpected, because unobservably beneficial locations with better first nature attract homeless persons, presumably causing an upward bias of the estimated coefficient of the agglomeration variable. We interpret the downward bias found in this instrumented result as follows: unobservably beneficial places with attractive first nature are strictly managed and controlled by local administrators so as not to be

---

<sup>41</sup>We also constructed an instrumental variable based on 50-*m* and 10-*m* divergences from the river line. However, instrumental variables based on such smaller divergence did not show sufficient relevance (i.e., the first stage F-statistics are small). In addition, simultaneously including all instrumental variables is not supported by the overidentification test. Therefore, we used only an instrumental variable based on a 100-*m* divergence from the river shore.

inhabited by homeless persons informally. Less advantageous locations are relatively freely available for them, and such disadvantageous locations are easier for them to illicitly occupy, which can lead to the downward bias of the coefficient of the cluster-size variable.

## 5 Robustness Checks Related to the Drone Data

This section deals with some concerns related to the drone data. In addition, we consider different expression of cluster sizes. We thereby replace a cluster-size variable with that expresses the affluence of each cluster, basically captured by the sum of house temperatures by cluster.

### 5.1 Houses with Roofs Fully Visible

As is already mentioned in Section 3.1, some of the houses have roofs covered by tree edges and leaves. In the baseline analysis, to maintain the sample size, we constructed a house temperature variable by averaging thermal information over the visible area of the house polygon from the sky, and we did not drop houses whose roofs are partly covered by vegetation from the sample. In this fashion, however, the invisible roof area may show much higher or lower temperature than the visible area does, leading to an imprecise measure of the house temperature. To overcome this, we only exploit the houses whose roofs are fully visible in the daytime aerial pictures, at the expense of losing observations.

Table 3 shows the result.

[Table 3 around here]

After limiting the sample to houses with fully visible roofs, the number of observations reduces to 111 from 160, which is a substantial decline. Despite this drop of the number of observations, the result displayed in Table 3 corroborates the significantly positive effect of the cluster size on the house temperature, both in the specification with  $N(i)_{-i}$  for column (2) and  $DN(i)_{-i}$  for column (4).

### 5.2 Different Choice of House Temperature Variable

Despite its instability as a measure of house temperature compared to the average value of the temperatures within house polygons, the maximum value of the house temperature for each house polygon, such as the most reddish part in Figure 1b, may better represent the inside temperature.<sup>42</sup> To see if

---

<sup>42</sup>For instance, if heat-producing objects such as birds and small animals are on the roof, the maximum inside house temperature measured from outside may capture these outside heat sources. Moreover, when the analysis is based on the

the results remain unchanged, we adopt the highest value of house temperature instead of the average value as our dependent variable. To alleviate the concern that the part not covered by edges and leaves shows the highest temperature over the roof polygon, we conduct the same regression based on the sample of houses with fully visible roofs.

Table 4 shows the results.

[Table 4 around here]

Columns (1) and (2) are for  $N(i)_{-i}$ , and columns (3) and (4) for  $DN(i)_{-i}$ , with the full sample; and columns (5) and (6) are for the  $N(i)_{-i}$  specification, and columns (7) and (8) for the  $DN(i)_{-i}$  specification, with the subsample of houses perfectly visible. The RE results based on the cluster size (column (1) for  $N(i)_{-i}$  and column (3) for  $DN(i)_{-i}$ ) are insignificant, despite being positive, as expected. Regarding the results of the REIV, both specifications show significantly positive coefficients on the agglomeration variable at the 5% level. RE results may be insignificant because the roof part showing the highest temperature was invisible from the drone, as the results based on the sample of houses with roofs fully visible are all significant at the 1% level (columns (5)–(8)).

### 5.3 Different Cluster-Size Variable (Sum of House Temperatures)

We consider a variable expressing the aggregate living standards of each cluster, not just the cluster size itself. The idea is that a homeless person may be better off if homeless persons in their neighborhood live relatively well. We calculate the sum of house temperatures in cluster  $C(i)$ , exclusive of house  $i$ 's contribution. Assuming that house temperatures in the winter express how well-off homeless persons are, the sum of temperatures of houses in a cluster may represent the overall living standards in that cluster. However, the sum should be corrected due to the missing values for some houses, as explained in Section 3.1. Therefore, we propose an adjusted version of the sum of temperatures of houses in cluster  $C(i)$  that replaces missing temperature values with the average of the observed house temperatures in cluster  $C(i)$ . The variable is computed as follows:

$$ST_{-i}(i) \equiv \sum_{j \in C'(i) \setminus \{i\}} T_j + \sum_{j \in C(i) \setminus C'(i)} \bar{T}_{C'(i)} = \sum_{j \in C'(i)} T_j + \sum_{j \in C(i) \setminus C'(i)} \bar{T}_{C'(i)} - T_i = ST(i) - T_i,$$

---

full sample, employing the highest temperature over the house polygons may be less adequate because of the possibility that a roof part hidden by leaves and edges reveals the highest roof temperature of a house. To circumvent such mistakes in collecting house temperature data, we use the average temperature value rather than an extreme value, such as the highest temperature within a house polygon.

where  $T_j$  is the temperature of house  $j$ ,  $C'(i)$  is the subset of houses in cluster  $C(i)$  whose house temperatures were observed,  $N'(i)$  is the number of houses in the set of houses in  $C'(i)$ ,

$$\bar{T}_{C'(i)} \equiv \frac{1}{N'(i)} \sum_{j \in C'(i)} T_j,$$

which is the average temperature of houses whose temperatures were observed, and

$$ST(i) \equiv \frac{N(i)}{N'(i)} \sum_{j \in C'(i)} T_j,$$

which expresses the total affluence of cluster  $C(i)$ . This index is computed by assuming that the missing house temperatures are, on average, equal to non-missing house temperatures in the same cluster.

As in the case of  $N(i)_{-i}$  and  $DN(i)_{-i}$ , the distance-discounted version of  $ST(i)_{-i}$  can also be considered:

$$DST_{-i}(i) \equiv \sum_{j \in C'(i) \setminus \{i\}} e^{-d_{ij}} T_j + \sum_{j \in C(i) \setminus C'(i)} e^{-d_{ij}} \bar{T}_{C'(i)} = DST(i) - T_i,$$

where

$$DST(i) \equiv \sum_{j \in C'(i)} e^{-d_{ij}} T_j + \sum_{j \in C(i) \setminus C'(i)} e^{-d_{ij}} \bar{T}_{C'(i)}.$$

The left and right panels in Figure 6, respectively, display the relationship between  $ST(i)_{-i}$  and  $DST(i)_{-i}$  and the house temperature.

[Figure 6 around here]

A casual observation of the graph reveals a positive correlation between the cluster-affluence measured by the sum of house temperatures by cluster and the house temperature.

Turning to the results in Table 5, which are based on the choice of  $ST(i)_{-i}$  and  $DST(i)_{-i}$  with a replacement of  $N(i)_{-i}$  and  $DN(i)_{-i}$ , the coefficient on the cluster-affluence variable is significantly positive at least at the 5% level in all columns.

[Table 5 around here]

Under the choice of  $ST(i)_{-i}$  and  $DST(i)_{-i}$ , we interpret the magnitude of the coefficients as follows: For the result based on  $ST(i)_{-i}$ , 1°C increase in the sum of house temperatures of a cluster increases

the temperature of a house belonging to the cluster by 0.124°C. An analogous interpretation can be applied to the result of  $DST(i)_{-i}$ . As for the first stage F-statistic, the full sample analysis does not show a sufficient relevance (columns (2) and (4)), but the analysis with the sample limited to houses whose roofs are fully visible satisfies relevance.<sup>43</sup>

Despite this successful results of  $ST(i)_{-i}$  and  $DST(i)_{-i}$ , we propose some comments on the undesired aspects of  $ST(i)_{-i}$  and  $DST(i)_{-i}$  as the measure of the affluence level of a cluster. First, the summation of house temperatures over a cluster is subject to the replacement of missing house temperatures  $T_{j \in C(i) \setminus C'(i)}$  with  $\bar{T}_{C'(i)}$ . However, this replacement may not be ideal for clusters with the relatively large number of houses lacking temperature values.

Moreover, the house temperature values themselves capture aspects related to both living standards and to such aspects as the natural conditions at the time of data collection. Simply summing house temperatures without accounting for factors not related to living standards may not produce an accurate representation of the overall living standards for each cluster. Thus, we utilize simpler but more-secure measures for the cluster size variable, such as  $N(i)_{-i}$  and  $DN(i)_{-i}$ , in the following section.

## 6 Other Robustness Checks

This section presents other robustness checks. Due to the ambiguity of how to define the cluster affluence variable, we stick to the choice of cluster size variables,  $N(i)_{-i}$  and  $DN(i)_{-i}$ , in this section.<sup>44</sup>

### 6.1 House Size (Floor Area)

Floor area may have two opposite effects on house temperature. On the one hand, it may be more difficult to heat the whole house if the house floor area is large. Thus, a larger floor area may lower the house temperature. On the other hand, more well-off homeless persons may live in larger houses, which can lead to a positive correlation between house floor area and temperature. Table OA3 in the online appendix presents the results when additionally controlling for the house floor size. The results obtained show robustness, both under the choice of  $N(i)_{-i}$  and  $DN(i)_{-i}$ .<sup>45</sup>

---

<sup>43</sup>We also conducted estimations for  $ST(i)_{-i}$  and  $DST(i)_{-i}$ , based on the choice of the maximum house temperature over the house polygon as the house temperature measure. Similar results to those displayed in this section were found. See Table OA2 in the online appendix.

<sup>44</sup>Results based on  $ST(i)_{-i}$  and  $DST(i)_{-i}$  are robust although not displayed. The results are available upon request.

<sup>45</sup>In all specifications, the variable of house floor area is insignificant and indistinguishable from zero, possibly because the opposing effects of the house floor area cancel each other out.

## 6.2 Number of Supermarkets

This robustness check accounts for the effect of the number of supermarkets near the houses. As mentioned in Section 2, homeless persons in our study area rarely beg for food or money. Instead, they earn money and buy food. Moreover, it is rare for free meals to be provided at the riverbank in our study area. Division of Health & Welfare in Kawasaki City (2019) report that one of the worries for homeless persons is food deficiency. Better access to supermarkets (especially those selling food at discounted prices) in their neighborhood improves their living standards by decreasing food expenditures.<sup>46</sup> We control for access to (inexpensive) food by adding a variable representing the number of supermarkets near the houses. The significantly positive coefficients on  $N(i)_{-i}$  and  $DN(i)_{-i}$  are robustly corroborated (Table OA4 in the online appendix).<sup>47</sup>

## 6.3 Number of Scrap Firms

On the income side, we include the number of scrap firms reachable for the homeless persons. As mentioned in Section 2, homeless persons' incomes mainly come from illegally collecting cans and metal scrap and conducting illicit transactions with scrap firms. After controlling for the number of scrap firms near the houses, the significant and positive effects of the cluster size variables are found to be robust (Table OA5 in the online appendix).<sup>48</sup>

## 6.4 Distance to Nisshin Town

We consider another possible type of earnings. The majority of homeless persons rely on earnings from can or metal scrap collection, but some earn money by temporarily working in the construction sector. To take into account this possibility, we include the distance to Nisshin Town in the model. Nisshin Town provides informal job opportunities for daily construction workers and is approximately 7 km from the southeast end of our study area. Our featured variables,  $N(i)_{-i}$  and  $DN(i)_{-i}$ , have a significant positive effect on house temperature in this robustness check (Table OA6 in the online appendix).<sup>49</sup>

---

<sup>46</sup>Indeed, Suzuki (2008) interprets a higher density of supermarkets as better access to food for homeless persons in Osaka, Japan.

<sup>47</sup>For more comments on the supermarket variable, see the online appendix.

<sup>48</sup>For additional comments on the scrap firm variable, see the online appendix.

<sup>49</sup>Additional discussions on the Nisshin Town variable are provided in the online appendix.

## 6.5 Vegetation Coverage

In the baseline model, we choose a 5- $m$  buffer range for vegetation coverage. In this robustness check, we change the buffer range to 10  $m$  and 15  $m$  to find that the positive impact of  $N(i)_{-i}$  and  $DN(i)_{-i}$  remains unchanged (Table OA7 in the online appendix).

## 6.6 Wind Speed Effect

We consider the effect of wind speed at the time of the collection of house temperature data. However, after including the wind-speed variable, the result remains unchanged (Table OA8 in the online appendix).<sup>50</sup>

## 6.7 Effect of Bridges

As mentioned in Section 3.1, we cannot collect data for houses located underneath bridges, because these are inaccessible for drones.<sup>51</sup> However, the houses of homeless persons may be located underneath bridges and are thus invisible in the aerial images. To address this point, we exclude houses close to bridges and repeat the estimation. In addition, we conduct an analogous estimation by dropping all houses in a cluster that contains houses sufficiently close to bridges. The results are robust for both approaches to dropping observations near bridges. (Columns (1)–(8) in Table OA9 in the online appendix).<sup>52</sup>

## 6.8 Effect of Houses on the Opposite Shore

As displayed in Figure 4c, houses of homeless persons are located on opposite shores of the river, implying possibility of interaction between homeless persons located on the opposite shores. Because this is only possible by crossing a pedestrian bridge, we exclude houses sufficiently close to pedestrian bridges in the study area. As shown in Figure 4b, there are three pedestrian bridges in the study area, so we drop house observations near each.

The first-stage F-statistic in Columns (10) and (12) in Table OA9 is not sufficiently high in this robustness check. The positive significance of the cluster-size variable are weaker than other robustness checks but still significant at the 10% and 5% levels for the  $N(i)_{-i}$  and  $DN(i)_{-i}$  specifications

---

<sup>50</sup>How to construct the wind-speed variable and an additional discussion appear in the online appendix.

<sup>51</sup>Figure 4b shows bridges (both pedestrian and non-pedestrian bridges) in the study area.

<sup>52</sup>How to keep only the subsample sufficiently far from bridges is explained in the online appendix.



(Columns (9)–(12) in Table OA9 in the online appendix).<sup>53</sup>

## 7 Discussion on the Thermal Data and the Experiment for Data Validation

This section discusses two concerns about the use of thermal data and defends its validity by showing the thermal data recorded in the thermal experiment we conducted. The first concern is the seemingly low values of house temperatures recorded by the drone, addressed in Section 3.5. The second concern is the possibility of heat radiation from neighboring houses, addressed in Section 4.1.

The thermal experiments should corroborate the following: (i) whether the indoor temperature is sufficiently high for a person to stay inside and (ii) whether heat radiation from a house is only limited to a spatially narrow range. We resolve the two concerns based on thermal data we collected in an experiment in which we built an imitation of a typical house in the study area.

### 7.1 Thermal Experiment

The experiment to replicate the thermal data collected in the study area was conducted in the evening of December 9, 2022. The experiment site was a private drone field located in Kanagawa Prefecture (this includes our study area), and the ground was covered by grass, similar to the natural conditions on the riverbank.<sup>54</sup> We temporarily built a simplified replica of a house similar to those found in our study area. The replica house had sides equal to 3 *m* and a height equal to 2.2 *m*.<sup>55</sup> We covered the framework of the house with blue plastic sheets for its exterior and duckboards on the ground as a floor. Also, the interior thin walls and floor were covered by cardboard.<sup>56</sup> For a heat origin inside the replica house, we put two portable electric heaters and two volume mobile batteries. For pictures of our replica house, see Figure OA5 in the online appendix.

Analogous to the data collection method in the study area, we conducted drone flights and took aerial and thermal images of the replica house. Figure 7a is the aerial picture of the house taken by the drone before the sunset, and Figure 7b is the thermal image we took at 19:15.

[Figure 7 around here]

---

<sup>53</sup>For more discussions about this robustness check, see the online appendix.

<sup>54</sup>We rented Sagamiko Drone Field.

<sup>55</sup>Due to the limited rental time of the drone field, we put up a ready-made tent framework whose size was similar to the average house size observed in the study area, and then modified it.

<sup>56</sup>We thank Nairu Kimura for kindly sharing his experience when he visited a house of a homeless person on the riverbank of the Tama River. Referring to his video and pictures printed in Murata (2015), we built the replica.

We conducted drone flights and took thermal pictures with 3-min intervals. The time range when the drone filmed the thermal images was 18:12–19:24, but the 18:51 thermal image was missing due to a drone battery exchange. The same drone and thermal camera as used in the actual data collection in the study area, the Matrice 210 drone with the thermal Zenmuse-XT2 camera, were used for the flight campaign, and the altitude of the drone was 140 *m*. From the thermal and aerial images, we calculate the average temperature over the house polygon, with which we define the house temperature recorded by the drone.

We collected the inside and outside temperatures of the replica house with five portable thermometers that can digitally log temperature values every 10 sec. Two thermometers were set inside the house; one was set near the ceiling, and the other on the floor. The other three thermometers were set at different locations outside; immediately outside the exterior wall of the replica house, 1.5 *m* apart from the wall, and 3.0 *m* apart from it. The recorded temperatures were converted to 3-min-level data by averaging 18 values of a 10-sec interval.

## 7.2 Thermal Data Validation

Based on the temperature data collected in the experiment, we investigate whether the inside temperature is sufficiently high even when the house surface temperature recorded by the drone is low. To begin, we confirm the similarity between the actual and experimental temperatures. Table 6 compares the house temperatures collected in the experiment and those on the riverbank.

[Table 6 around here]

Column (1) in Table 6 corresponds to the recorded temperatures in the experiment, and columns (2)–(4) correspond to the actual data by date. “Drone (Raw)” displays the house roof temperature recorded by drone, “Outside” displays the outside temperature at the same record time as the drone temperature, and “Drone (Adjusted by the outside temperature)” is defined as the “Drone (Raw)” minus “Outside” temperatures. The values in Table 6 are averages of observations for each date.

The raw drone temperatures in the experiment (column (1)) and the actual data (columns (2)–(4)) do not show comparable values. If adjusted by the outside temperatures, however, they are comparable ( $-8.372^{\circ}\text{C}$  for the experimental data; while  $-9.779^{\circ}\text{C}$ ,  $-9.307^{\circ}\text{C}$ , and  $-7.512^{\circ}\text{C}$  for the actual data), suggesting the reliability of our thermal experiment.

Based on the validity of our experiment from the discussion above, we next make a comparison

between the indoor temperatures and those recorded from outside by drone flights.

[Figure 8 around here]

Figure 8 shows time series plots of the recorded temperatures. From an instant observation of the plots in Figure 8, indoor temperatures are much higher than the house temperatures recorded by the drone. Comparing the indoor temperatures (those on the ceiling depicted by navy plots and those on the floor by red plots) and the roof temperature recorded by the drone (those marked with orange plots), the drone temperatures are much lower than the indoor temperatures. This means that house temperature data we collected in the winter of 2019 was not unnaturally low.

Another important observation from Figure 8 is the apparent positive relationship between the indoor temperatures and the drone temperature. It can be safely asserted that a higher drone temperature is accompanied by a higher indoor temperature because (i) the only heat source was the heaters set in the replica house, (ii) the outside temperature plotted by green triangle marks exhibits a slight decline as the experiment time passes, (iii) the indoor temperature plotted by navy or red marks rises through time, and (iv) the drone temperature plotted by orange squares shows an increasing behavior, reflecting the heat inside the house. This finding supports the assumption that the higher the indoor temperature is, the higher the house temperature indirectly sensed from outside.<sup>57</sup>

### 7.3 Heat Radiation

Turning to the second issue in regard with whether heat radiation from a house is limited to a narrow geographic area, we utilize the temperature data recorded by thermometers. For this exercise, temperature values recorded by thermometers are aggregated at a minute level.

Figure 9 plots the temperatures by minute.

[Figure 9 around here]

Blue cross marks depict the temperature by minute at each location where the thermometers were set (the ceiling and floor inside the imitation house; and 0, 1.5, and 3.0 *m* apart from the house exterior wall). Red circles are the mean temperatures at each location.

From a quick look at the figure, high indoor temperature immediately drops at outside locations, suggesting that heat radiation across houses seems to rarely occur. Hence, at least from our experiment, it is reasonable to assume that heat radiation is limited to a narrow spatial range and that a

---

<sup>57</sup>In addition, we display a graph showing the positive relationship between the drone temperature and the indoor temperature in Figure A2 in the Appendix.

house temperature is not affected by the temperatures of neighboring houses through the channel of heat radiation.

## 8 Conclusion

In this paper, we investigated how homeless persons benefit from living in clusters via a channel of social interactions with those located in the same cluster. Starting from a casual observation that cage-like houses built by homeless persons are distributed in clusters on the riverbank along the Tama River near Tokyo, we hypothesized that homeless individuals enjoy benefits by living close to other homeless persons.

To examine our hypothesis, we identified the locations of houses of homeless persons based on aerial images captured by a drone. The detection of house locations was possible due to the characteristics of homeless persons on the riverbank (i.e., not nomadic but settled in fixed locations). By investigating aerial images, we identified house-like objects characterized by unique features. Based on the house locations, we calculated the distances between houses. After grouping houses into clusters via single-linkage clustering, we used the house location and distance data to estimate the impact of being located in a larger cluster on the living standards of homeless persons, measured using house temperatures during the winter. Our estimation results showed that if a house is located in a larger cluster, its house temperature is higher, indicating that a homeless person living in a larger cluster is better off.

The naive estimates may suffer from an endogeneity problem due to the cluster-size variable (our featured variable, measuring the extent of social interactions among homeless persons). Specifically, there are two sources of endogeneity related to cluster size: unobservable individual-specific characteristics and unobservable location-specific characteristics. The former induces downward bias in the positive coefficient of cluster size because unobservably less-able or more-disadvantaged homeless persons may sort into larger clusters to seek greater support from peers. This type of endogeneity could be resolved by eliminating the individual fixed effects. This solution, however, was not possible in our dataset because cluster size is time-invariant. The expected bias direction of the coefficient on cluster size in the naive estimation without addressing unobservable individual-specific characteristics may be negative due to negative sorting to larger clusters.

In terms of the endogeneity due to unobservable location-specific characteristics, we use an instrumental variable, the inner/outer curve dummy variable in order that flatter spaces are generated on the inner curve of the river due to sedimentation. Thus, areas located on the inner curve should be

more suitable for building houses than those located in the outer curve, which leads to larger clusters of houses on the inner curve. The instrumented result again shows that homeless persons benefit from being located in larger clusters.

By combining the expectation that unobservable individual-specific characteristics induce downward bias and the finding of the positive coefficient of cluster size in the IV result, we expect to find a positive impact of cluster size on the house temperature. Thus, it is concluded that homeless persons benefit from living close to other homeless persons. Residential proximity enables homeless persons to interact with each other, and these social interactions can improve standards of living.

The last part of this paper discussed the validity of the thermal data recorded via drone flights. To this end, we conducted a thermal experiment in which we replicated the environment of the study area. Comparing the thermal data collected in the experiment and those collected in the study area, we reasonably corroborated the validity of the roof temperature recorded by the thermal infrared camera carried by the drone.

What is most innovative in this paper is that, to the best of our knowledge, it is the first to measure the living standards of individuals, using thermal information collected by a drone loaded with a thermal sensor. Such an indirect sensing method has been only recently introduced to natural sciences. Applying this new technique to social sciences enlarges the possibility of knowing pieces of information that have long been hard to access by researchers. The idea of measuring welfare levels by thermal data and the introduction of interdisciplinary data collection methods may open the door to a new era of social science research with wider perspectives.

## References

- AKIYAMA, Y., K. IIZUKA, O. YACHIDA, AND S. SUGITA (2019): “Fundamental Research on Estimating the Vacant Houses using Thermal Infrared and Visible Imagery Observed from Unmanned Aerial Vehicle (UAV),” *Proceedings of the 28th Annual Meeting on Geographic Information Systems Association of Japan (in Japanese)*, F-2-3.
- ALLGOOD, S. AND R. S. WARREN JR (2003): “The Duration of Homelessness: Evidence from a National Survey,” *Journal of Housing Economics*, 12, 273–290.
- BALARAS, C. A. AND A. ARGIRIOU (2002): “Infrared Thermography for Building Diagnostics,” *Energy and Buildings*, 34, 171–183.
- BAYER, P., S. L. ROSS, AND G. TOPA (2008): “Place of Work and Place of Residence: Informal Hiring Networks and Labor Market Outcomes,” *Journal of Political Economy*, 116, 1150–1196.
- BRUECKNER, J. K. (2013): “Slums in Developing Countries: New Evidence for Indonesia,” *Journal of Housing Economics*, 22, 278–290.
- CALÍNSKI, T. AND J. HARABASZ (1974): “A Dendrite Method for Cluster Analysis,” *Communications in Statistics-theory and Methods*, 3, 1–27.
- CANAY, I. A., A. SANTOS, AND A. M. SHAIKH (2021): “The Wild Bootstrap with a “Small” Number of “Large” Clusters,” *Review of Economics and Statistics*, 103, 346–363.
- COBB-CLARK, D. A., N. HERAULT, R. SCUTELLA, AND Y.-P. TSENG (2016): “A Journey Home: What Drives How Long People Are Homeless?” *Journal of Urban Economics*, 91, 57–72.
- COMBES, P.-P., G. DURANTON, AND L. GOBILLON (2011): “The Identification of Agglomeration Economies,” *Journal of Economic Geography*, 11, 253–266.
- COMBES, P.-P., G. DURANTON, L. GOBILLON, AND S. ROUX (2010): “Estimating Agglomeration Economies with History, Geology, and Worker Effects,” in *Agglomeration Economics*, ed. by E. L. Glaeser, Oxford, UK: Oxford University Press, 15–66.
- CORINTH, K. AND D. S. LUCAS (2018): “When Warm and Cold Don’t Mix: The Implications of Climate for the Determinants of Homelessness,” *Journal of Housing Economics*, 41, 45–56.

- CULHANE, D. P. (2010): “Tackling Homelessness in Los Angeles’ Skid Row: The Role of Policing Strategies and the Spatial Deconcentration of Homelessness,” *Criminology & Public Policy*, 9, 851–857.
- DIVISION OF HEALTH & WELFARE IN KAWASAKI CITY (2019): “Project for Supporting the Homeless to be Independent (2019–2023) (in Japanese),” .
- EARLY, D. W. (2005): “An Empirical Investigation of the Determinants of Street Homelessness,” *Journal of Housing Economics*, 14, 27–47.
- FELER, L. AND J. V. HENDERSON (2011): “Exclusionary Policies in Urban Development: Under-servicing Migrant Households in Brazilian Cities,” *Journal of Urban Economics*, 69, 253–272.
- FISHER, W. D. (1958): “On Grouping for Maximum Homogeneity,” *Journal of the American Statistical Association*, 53, 789–798.
- HALPIN, B. (2016): “Cluster Analysis Stopping Rules in Stata,” *University of Limerick Working Paper*, WP2016-01.
- HELLERSTEIN, J. K., M. MCINERNEY, AND D. NEUMARK (2011): “Neighbors and Coworkers: The Importance of Residential Labor Market Networks,” *Journal of Labor Economics*, 29, 659–695.
- ITO, K., S. MORIKAWA, T. OKAMURA, K. SHIMOKADO, AND S. AWATA (2014): “Factors Associated with Mental Well-being of Homeless People in Japan,” *Psychiatry and Clinical Neurosciences*, 68, 145–153.
- IWATA, M. (2004): “Who Becomes Homeless? (in Japanese),” *Japan Labor Issues*, 49–58.
- IWATA, S. AND K. KARATO (2011): “Homeless Networks and Geographic Concentration: Evidence from Osaka City,” *Papers in Regional Science*, 90, 27–46.
- KIM, J. S., E. PATACCHINI, P. M. PICARD, AND Y. ZENOU (2017): “Urban Interactions,” *IFN Working Paper*, 1192.
- LALL, S. V., M. K. LUNDBERG, AND Z. SHALIZI (2008): “Implications of Alternate Policies on Welfare of Slum Dwellers: Evidence from Pune, India,” *Journal of Urban Economics*, 63, 56–73.
- LEE, B. A. AND T. PRICE-SPRATLEN (2004): “The Geography of Homelessness in American Communities: Concentration or Dispersion?” *City & Community*, 3, 3–27.

- MARMAROS, D. AND B. SACERDOTE (2006): “How Do Friendships Form?” *The Quarterly Journal of Economics*, 121, 79–119.
- MICHELL, D. AND K. BIGGS (1979): “Radiation Cooling of Buildings at Night,” *Applied Energy*, 5, 263–275.
- MORETTI, E. (2004): “Estimating the Social Return to Higher Education: Evidence from Longitudinal and Repeated Cross-Sectional Data,” *Journal of Econometrics*, 121, 175–212.
- MORIKAWA, S., R. UEHARA, K. OKUDA, Y. SHIMIZU, AND Y. NAKAMURA (2011): “Morbidity of Mental Illness among Homeless People in One Area of Tokyo (in Japanese),” *Japanese Journal of Public Health*, 58, 331–339.
- MURATA, R., ed. (2015): *Homeless Superstar Legends (in Japanese)*, Loft Books.
- NISHIO, A., R. HORITA, T. SADO, S. MIZUTANI, T. WATANABE, R. UEHARA, AND M. YAMAMOTO (2017): “Causes of Homelessness Prevalence: Relationship Between Homelessness and Disability,” *Psychiatry and Clinical Neurosciences*, 71, 180–188.
- OAKES, P. M. AND R. C. DAVIES (2008): “Intellectual Disability in Homeless Adults: A Prevalence Study,” *Journal of Intellectual Disabilities*, 12, 325–334.
- OKAMOTO, Y. (2007): “A Comparative Study of Homelessness in the United Kingdom and Japan,” *Journal of Social Issues*, 63, 525–542.
- OKAMURA, T., K. ITO, S. MORIKAWA, AND S. AWATA (2014): “Suicidal Behavior Among Homeless People in Japan,” *Social Psychiatry and Psychiatric Epidemiology*, 49, 573–582.
- OKAMURA, T., T. TAKESHIMA, H. TACHIMORI, K. TAKIWAKI, Y. MATOBA, AND S. AWATA (2015): “Characteristics of Individuals with Mental Illness in Tokyo Homeless Shelters,” *Psychiatric Services*, 66, 1290–1295.
- PHILIPPOT, P., C. LECOCQ, F. SEMPOUX, H. NACHTERGAEL, AND B. GALAND (2007): “Psychological Research on Homelessness in Western Europe: A Review from 1970 to 2001,” *Journal of Social Issues*, 63, 483–503.
- SALIZE, H. J., C. DILLMANN-LANGE, G. STERN, B. KENTNER-FIGURA, K. STAMM, W. RÖSSLER, AND F. HENN (2002): “Alcoholism and Somatic Comorbidity Among Homeless People in Mannheim, Germany,” *Addiction*, 97, 1593–1600.



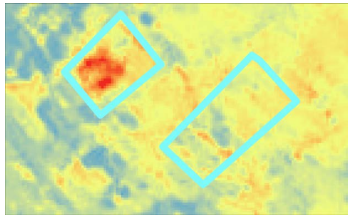
- SCHMUTTE, I. M. (2015): “Job Referral Networks and the Determination of Earnings in Local Labor Markets,” *Journal of Labor Economics*, 33, 1–32.
- SUGITA, S., N. KOBAYASHI, AND M. DOHI (2010): “The Movement of the Sleeping Places of Homeless People and Exclusion of those People (in Japanese),” *Journal of the City Planning Institute of Japan*, 45, 751–756.
- SUZUKI, W. (2008): “What Determines the Spatial Distribution of Homeless People in Japan?” *Applied Economics Letters*, 15, 1023–1026.
- TAKANO, T., K. NAKAMURA, S. TAKEUCHI, AND M. WATANABE (1999): “Disease Patterns of the Homeless in Tokyo,” *Journal of Urban Health*, 76, 73–84.
- TAKEUCHI, A., M. CROPPER, AND A. BENTO (2008): “Measuring the Welfare Effects of Slum Improvement Programs: The Case of Mumbai,” *Journal of Urban Economics*, 64, 65–84.
- VAN STRAATEN, B., C. T. SCHRIJVERS, J. VAN DER LAAN, S. N. BOERSMA, G. RODENBURG, J. R. WOLF, AND D. VAN DE MHEEN (2014): “Intellectual Disability Among Dutch Homeless People: Prevalence and Related Psychosocial Problems,” *PLoS One*, 9.
- WOLCH, J. R., A. RAHIMIAN, AND P. KOEGEL (1993): “Daily and Periodic Mobility Patterns of the Urban Homeless,” *The Professional Geographer*, 45, 159–169.
- YAMAKITA, T. (2006): “Comradeship within Communities of Homeless People (in Japanese),” *Japanese Sociological Review*, 57, 582–599.

## Figures and Tables

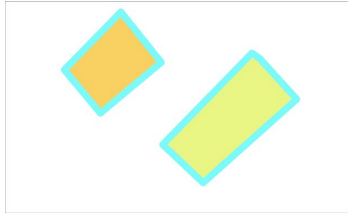
### Figures



(a) Sample of houses (orthophoto)



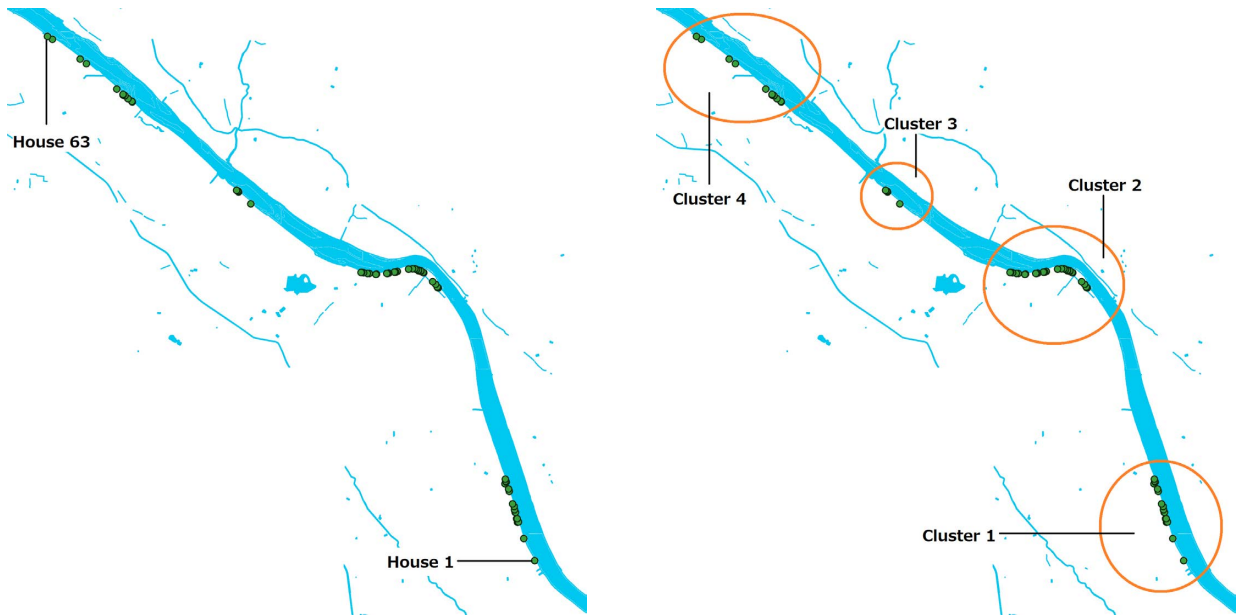
(b) Sample of thermal images



(c) Sample of average house temperatures

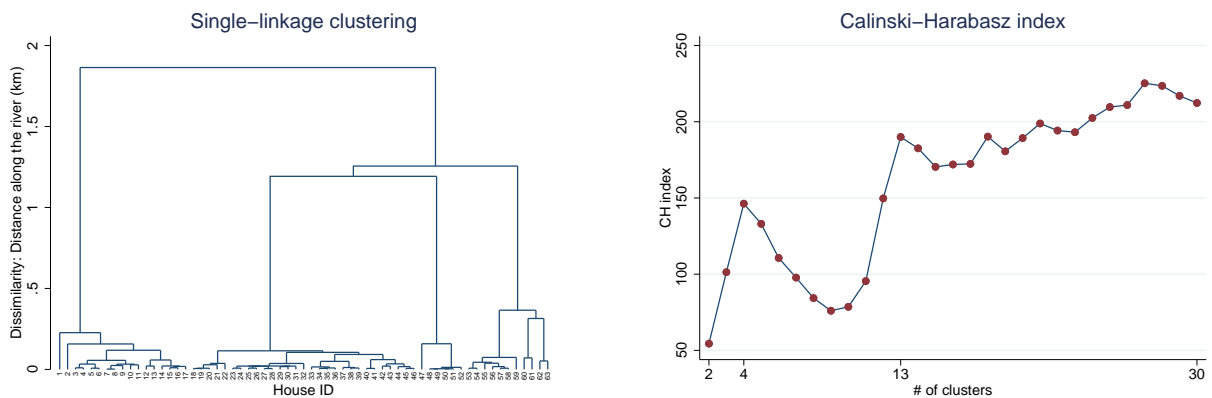
Figure 1: House polygons and temperatures

Figure 1a: Polygons marked with light blue lines are detected houses on February 17, 2019. Figure 1b: Polygons marked with light blue lines correspond to the detected houses in Figure 1a. Reddish (bluish) area indicates higher (lower) temperatures. Temperature is measured in  $^{\circ}\text{C}$ . Data was collected on February 17, 2019. Figure 1c: Polygons marked with light blue correspond to the detected houses in Figure 1c. Each polygon is colored by the average temperature within each polygon area. Data was collected on February 17, 2019.



(a) Location of house centroids in the whole study area  
 In both panels in Figure 2, light blue ribbon running from the southeast to the northwest is the river. Other light blue lines are ditches. Green points depict houses of the homeless persons.

Figure 2: House locations and clusters

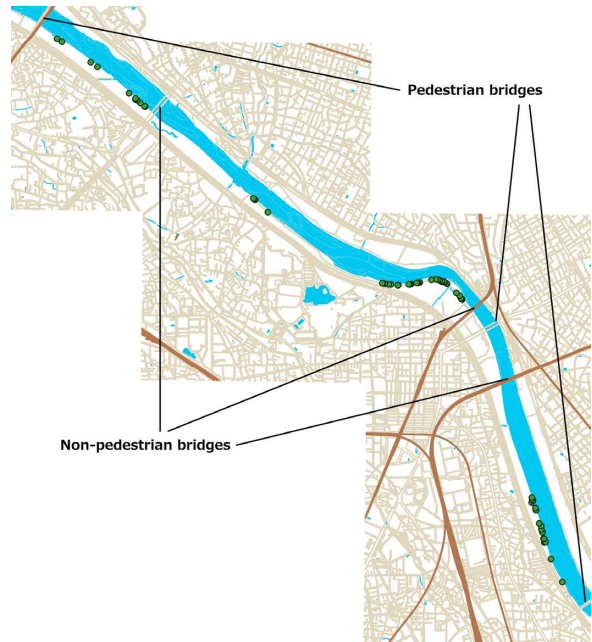


(a) Dendrogram based on single-linkage clustering  
 (b)  $CH$ -index in single-linkage clustering

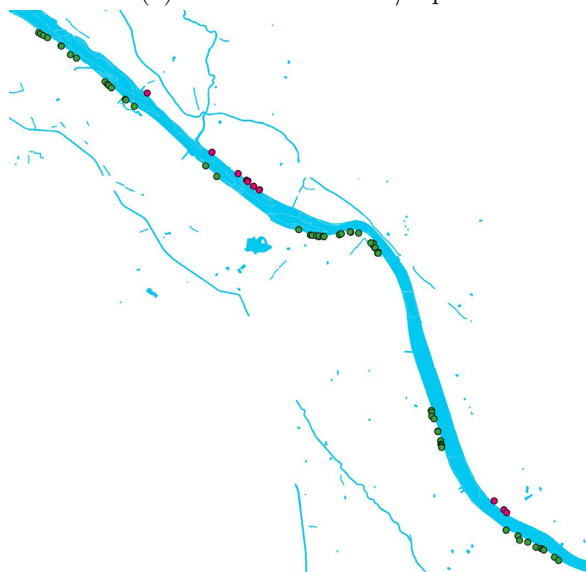
Figure 3: Single-linkage clustering and optimal number of clusters



(a) Houses and toilets/taps



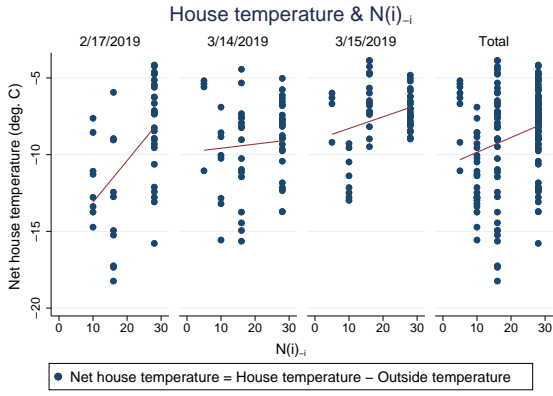
(b) Houses and bridges



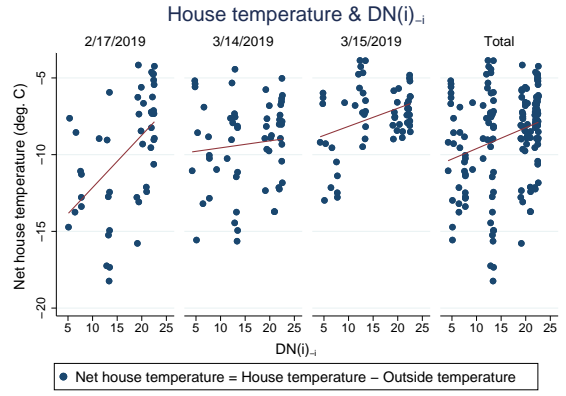
(c) Houses and inner/outer curves: Both sides of the river in 2020

Figure 4: Maps of the study area

Figure 4a: Light blue ribbon running from the southeast to the northwest is the river. Other light blue lines are ditches. Green points depict houses of the homeless persons. Yellow points depict toilets/taps. Figure 4b: Light blue ribbon running from the southeast to the northwest is the river. Other light blue lines are ditches. Green points depict houses of the homeless persons. Brown lines depict train rails. Beige lines depict roads. Figure 4c: Light blue ribbon running from the southeast to the northwest is the river. Other light blue lines are ditches. Green points depict houses of the homeless persons on Kanagawa(Kawasaki) side (the study area in February and March 2019). Pink points depict houses of the homeless persons on Tokyo side.



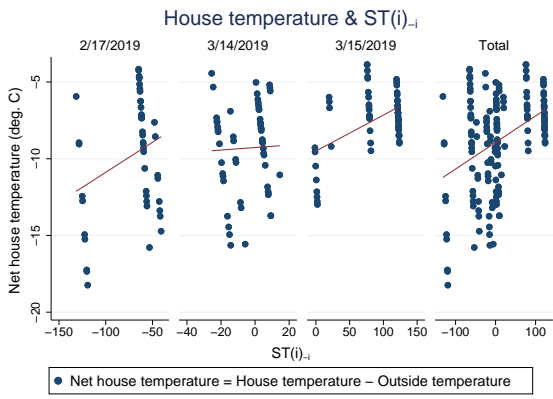
(a)  $N(i)_{-i}$  and house temperatures



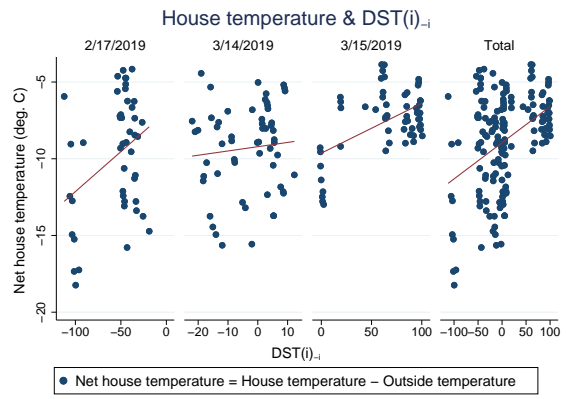
(b)  $DN(i)_{-i}$  and house temperatures

Figure 5: Cluster size and house temperatures

Both in Figures 5a and 5b, the vertical axis expresses “Net house temperature” defined by “House temperature recorded by the drone” minus “Outside temperature on the record time”. Red lines are linear fits.



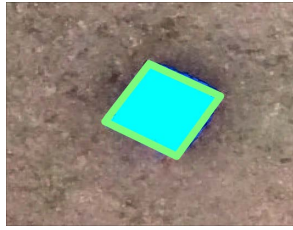
(a)  $ST(i)_{-i}$  and house temperatures



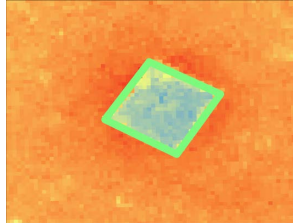
(b)  $DST(i)_{-i}$  and house temperatures

Figure 6: Cluster affluence and house temperatures

Both in Figures 6a and 6b, the vertical axis expresses “Net house temperature” defined by “House temperature recorded by the drone” minus “Outside temperature on the record time”. Red lines are linear fits.



(a) Aerial picture in experiment



(b) Thermal image in experiment (19:15)

Figure 7: Aerial and thermal images in experiment

Figure 7a: Polygon marked with light green lines is the replica house built for the thermal experiment on December 9, 2022. Figure 7b: Polygons marked with light green lines correspond to the replica house in Figure 7a. Reddish (bluish) area indicates higher (lower) temperatures. Temperature is measured in  $^{\circ}\text{C}$ . Data was collected at 19:15 on December 9, 2022.

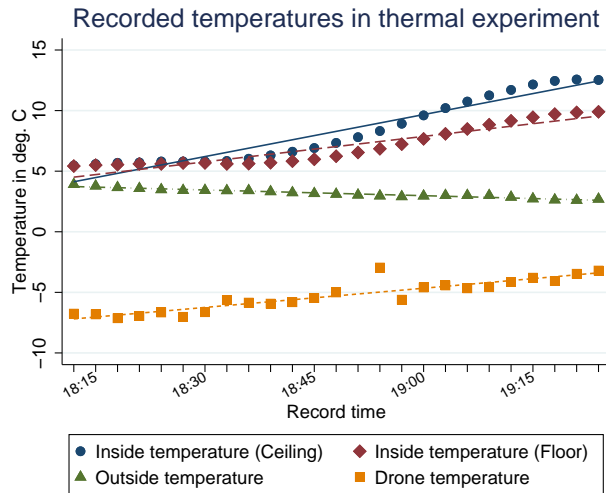


Figure 8: Recorded temperatures in thermal experiment (Drone, outside, inside)

Figure 8 shows time series of recorded temperatures in the thermal experiment on December 9, 2022. Inside temperatures (ceiling and floor) and outside temperature were recorded every 10 sec by thermal loggers and converted to data with 3-min intervals by taking averages by 3 min. Outside temperature was recorded at a point 3.0 m apart from the house exterior wall. Drone temperature was recorded every 3 min. The record corresponding to 18:51 was missing due to a battery exchange of the drone. Straight lines are linear fits for each temperature plot.

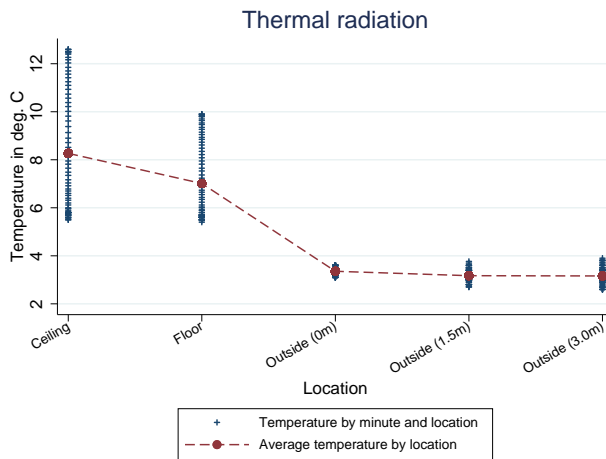


Figure 9: Thermal radiation in experiment

In Figure 9, inside (ceiling and floor) and outside temperatures were recorded by thermal loggers in the thermal experiment on December 9, 2022. Temperature data were recorded every 10 sec by thermal loggers and converted to data with 1-min intervals by taking averages by 1 min.

## Tables

Table 1: Summary Statistics

	Obs.	Mean	Std.Dev	Min	Max
<b>House temperature variables</b>					
House temperature (avg, deg. C)	160	0.219	4.301	-12.800	7.500
House temperature (max, deg. C)	160	2.112	3.864	-11.100	9.300
<b>Cluster size variables</b>					
$N(i)_{-i}$	160	20.850	7.995	5	28
$DN(i)_{-i}$	160	15.889	6.164	4.228	22.570
$ST(i)_{-i}$ (avg)	160	8.079	70.811	-131.590	123.857
$DST(i)_{-i}$ (avg)	160	6.508	54.821	-112.300	100.673
$ST(i)_{-i}$ (max)	160	45.026	67.164	-93.700	158.171
$DST(i)_{-i}$ (max)	160	34.298	51.960	-80.480	127.596
$ST(i)_{-i}$ (avg, roof fully visible)	160	-7.511	67.654	-146.748	100.147
$DST(i)_{-i}$ (avg, roof fully visible)	160	-5.358	51.264	-113.421	79.862
$ST(i)_{-i}$ (max, roof fully visible)	160	27.347	62.614	-107.112	131.136
$DST(i)_{-i}$ (max, roof fully visible)	160	20.639	47.547	-81.838	104.213
<b>Other variables</b>					
Inner/outer curve (1 if inner, 0 if outer)	160	0.487	0.501	0	1
Outside temperature (deg. C)	160	9.022	2.218	5.438	11.796
Distance to toilet/tap water ( $m$ )	160	310.229	153.581	58.327	632.955
Forest coverage (5 $m$ , %)	160	22.184	23.554	0	100
Forest coverage (10 $m$ , %)	160	20.914	18.582	0	84.753
Forest coverage (15 $m$ , %)	160	16.727	14.788	0	63.718
Grass coverage (5 $m$ , %)	160	62.391	22.968	0	100
Grass coverage (10 $m$ , %)	160	64.465	19.465	9.280	97.844
Grass coverage (15 $m$ , %)	160	64.460	18.999	8.735	97.835
Distance to the river shore ( $m$ )	160	18.745	8.681	4.875	42.867
House floor area ( $m^2$ )	160	11.594	7.415	2.437	35.638
Distance to Nisshin Town ( $km$ )	160	7.344	1.738	4.594	10.969
Wind speed ( $m/s$ )	160	3.964	0.748	2.275	5.116
Number of supermarkets (1 $km$ )	160	10.444	2.601	4	15
Number of scrap firms (2 $km$ )	160	8.919	3.715	3	13



Table 2: Baseline

Model:	(1)	(2)	(3)	(4)	(5)	(6)
Dependent variable:	POLS	RE	REIV	POLS	RE	REIV
	House Temperature (deg. C)					
$N(i)_{-i}$	0.100** (0.038)	0.092** (0.037)	0.195*** (0.067)			
$DN(i)_{-i}$				0.134** (0.053)	0.121** (0.051)	0.268*** (0.096)
Outside temperature (deg. C)	3.402*** (0.645)	2.947*** (0.521)	2.863*** (0.505)	3.491*** (0.674)	2.985*** (0.532)	2.930*** (0.521)
Distance to toilet/tap water ( $m$ )	-0.005** (0.002)	-0.005*** (0.002)	-0.007*** (0.002)	-0.004** (0.002)	-0.004** (0.002)	-0.006*** (0.002)
Forest coverage ( $5m$ , %)	0.072*** (0.016)	0.072*** (0.016)	0.069*** (0.015)	0.071*** (0.016)	0.072*** (0.016)	0.067*** (0.015)
Grass coverage ( $5m$ , %)	0.026 (0.017)	0.027 (0.017)	0.025 (0.017)	0.027 (0.017)	0.028 (0.017)	0.025 (0.017)
Distance to the river shore ( $m$ )	-0.067** (0.031)	-0.064** (0.028)	-0.100** (0.039)	-0.072** (0.031)	-0.067** (0.029)	-0.111** (0.045)
Date FE	Y	Y	Y	Y	Y	Y
Administrative division FE	Y	Y	Y	Y	Y	Y
# of observations	160	160	160	160	160	160
Adj R-sq	0.72			0.71		
Within R-sq		0.82			0.82	
Between R-sq		0.65			0.64	
Breusch and Pagan LM $\chi^2$		24.79			24.66	
[ p-val ]		0.00			0.00	
Sargan-Hansen stat. $\chi^2$		5.61			6.57	
[ p-val ]		0.06			0.04	
First stage						
Inner/outer curve (1 if inner, 0 if outer)			9.443*** (1.766)			6.859*** (1.393)
F-stat. (weak instrument)			28.60			24.24

Standard errors clustered by houses are in parentheses.

\*\*\*  $p < 0.01$ , \*\*  $p < 0.05$ , \*  $p < 0.1$

Table 3: Houses with roofs fully visible

	(1)	(2)	(3)	(4)
Sample:	Houses with roofs fully visible			
Model:	RE	REIV	RE	REIV
Dependent variable:	House Temperature (deg. C)			
$N(i)_{-i}$	0.212*** (0.055)	0.284*** (0.082)		
$DN(i)_{-i}$			0.297*** (0.087)	0.393*** (0.122)
Base control	Y	Y	Y	Y
Date FE	Y	Y	Y	Y
Administrative division FE	Y	Y	Y	Y
# of observations	111	111	111	111
Within R-sq	0.84		0.83	
Between R-sq	0.60		0.60	
Breusch and Pagan LM $\chi^2$	12.54		11.92	
[ p-val ]	0.00		0.00	
Sargan-Hansen stat. $\chi^2$	3.52		6.82	
[ p-val ]	0.17		0.03	
First stage				
Inner/outer curve (1 if inner, 0 if outer)		10.054*** (1.416)		7.273*** (1.120)
F-stat. (weak instrument)		50.42		42.20

Standard errors clustered by houses are in parentheses. Base control = Outside temperature, Distance to toilet/tap water, Forest and grass coverage (5-m buffers), Distance to the river shore.

\*\*\* p<0.01, \*\* p<0.05, \* p<0.1

Table 4: Maximum House Temperature within a House Polygon

Model:	(1)	(2)	(3)	(4)	(5)	(6)	(7)	(8)
	RE	REIV	RE	REIV	RE	REIV	RE	REIV
Sample:	Full				Houses with roofs fully visible			
Dependent variable:	House Temperature (maximum, deg. C)							
$N(i)_{-i}$	0.064 (0.040)	0.149** (0.067)			0.180*** (0.057)	0.255*** (0.076)		
$DN(i)_{-i}$			0.065 (0.059)	0.204** (0.098)			0.243*** (0.084)	0.353*** (0.115)
Outside temperature (deg. C)	3.754*** (0.541)	3.695*** (0.528)	3.772*** (0.549)	3.732*** (0.537)	4.151*** (0.588)	4.019*** (0.587)	4.258*** (0.610)	4.146*** (0.599)
Distance to toilet/tap water ( $m$ )	-0.004 (0.002)	-0.005** (0.002)	-0.003 (0.002)	-0.005** (0.002)	-0.008*** (0.002)	-0.009*** (0.002)	-0.008*** (0.002)	-0.009*** (0.002)
Forest coverage (5m, %)	0.057*** (0.015)	0.054*** (0.014)	0.057*** (0.016)	0.053*** (0.014)	0.058*** (0.020)	0.056*** (0.018)	0.054*** (0.021)	0.050*** (0.018)
Grass coverage (5m, %)	0.013 (0.016)	0.011 (0.016)	0.014 (0.016)	0.012 (0.016)	-0.005 (0.015)	-0.009 (0.014)	-0.005 (0.016)	-0.009 (0.015)
Distance to the river shore ( $m$ )	-0.055** (0.025)	-0.085** (0.039)	-0.052* (0.026)	-0.093** (0.045)	-0.068* (0.035)	-0.078 (0.049)	-0.077** (0.037)	-0.092* (0.055)
Date FE	Y	Y	Y	Y	Y	Y	Y	Y
Administrative division FE	Y	Y	Y	Y	Y	Y	Y	Y
# of observations	160	160	160	160	111	111	111	111
Within R-sq	0.80		0.80		0.82		0.82	
Between R-sq	0.59		0.58		0.60		0.60	
Breusch and Pagan LM $\chi^2$	21.76		22.50		9.81		9.93	
[ p-val ]	0.00		0.00		0.00		0.00	
Sargan-Hansen stat. $\chi^2$	4.01		4.51		2.53		4.50	
[ p-val ]	0.13		0.11		0.28		0.11	
First stage								
Inner/outer curve (1 if inner, 0 if outer)		9.444*** (1.766)		6.866*** (1.395)		10.046*** (1.419)		7.270*** (1.121)
F-stat. (weak instrument)		28.60		24.24		50.11		42.06

Standard errors clustered by houses are in parentheses. Base control = Outside temperature, Distance to toilet/tap water, Forest and grass coverage (5- $m$  buffers), Distance to the river shore.

\*\*\*  $p < 0.01$ , \*\*  $p < 0.05$ , \*  $p < 0.1$

Table 5: Choice of  $ST(i)_{-i}$  and  $DST(i)_{-i}$ 

Model:	(1)	(2)	(3)	(4)	(5)	(6)	(7)	(8)
Sample:	RE	REIV	RE	REIV	RE	REIV	RE	REIV
Dependent variable:	Full				Houses with roofs fully visible			
	House Temperature (deg. C)							
$ST(i)_{-i}$	0.017*** (0.005)	0.124** (0.063)						
$DST(i)_{-i}$			0.030*** (0.008)	0.132** (0.063)				
$ST(i)_{-i}$ (roof fully visible)					0.023*** (0.008)	0.171** (0.079)		
$DST(i)_{-i}$ (roof fully visible)							0.043*** (0.016)	0.194** (0.088)
Outside temperature (deg. C)	1.617*** (0.525)	-7.262 (5.345)	0.956* (0.538)	-5.828 (4.365)	1.610** (0.790)	-11.113 (7.094)	0.684 (1.076)	-9.644 (6.281)
Distance to toilet/tap water ( $m$ )	-0.004** (0.002)	-0.008*** (0.003)	-0.003** (0.001)	-0.005*** (0.002)	-0.004** (0.002)	-0.010*** (0.003)	-0.004** (0.002)	-0.007*** (0.002)
Forest coverage ( $5m$ , %)	0.075*** (0.017)	0.073*** (0.020)	0.074*** (0.017)	0.071*** (0.018)	0.076*** (0.026)	0.078*** (0.026)	0.077*** (0.026)	0.080*** (0.026)
Grass coverage ( $5m$ , %)	0.029 (0.018)	0.026 (0.021)	0.029 (0.018)	0.025 (0.019)	0.020 (0.019)	0.015 (0.021)	0.020 (0.019)	0.016 (0.020)
Distance to the river shore ( $m$ )	-0.041 (0.029)	-0.103 (0.065)	-0.048* (0.029)	-0.105* (0.061)	-0.044 (0.040)	-0.041 (0.067)	-0.045 (0.039)	-0.047 (0.066)
Date FE	Y	Y	Y	Y	Y	Y	Y	Y
Administrative division FE	Y	Y	Y	Y	Y	Y	Y	Y
# of observations	160	160	160	160	111	111	111	111
Within R-sq	0.82		0.83		0.84		0.84	
Between R-sq	0.62		0.62		0.49		0.50	
Breusch and Pagan LM $\chi^2$	30.11		31.83		18.71		19.90	
[ p-val ]	0.00		0.00		0.00		0.00	
Sargan-Hansen stat. $\chi^2$	9.21		8.70		15.88		13.97	
[ p-val ]	0.03		0.03		0.00		0.00	
First stage								
Inner/outer curve (1 if inner, 0 if outer)		15.132** (5.975)		14.234*** (5.065)		16.576*** (5.001)		14.631*** (4.231)
F-stat. (weak instrument)		6.41		7.90		10.99		11.96

Standard errors clustered by houses are in parentheses. Base control = Outside temperature, Distance to toilet/tap water, Forest and grass coverage ( $5m$  buffers), Distance to the river shore.

\*\*\*  $p < 0.01$ , \*\*  $p < 0.05$ , \*  $p < 0.1$

Table 6: Comparison between thermal data in experiment and actual data

Experimental/Actual:	(1)	(2)	(3)	(4)
	Experimental	Actual		
Site:	Drone field	Riverbank		
Date:	12/10/2022	2/17/2019	3/14/2019	3/15/2019
<b>Recorded temperatures (Mean, deg. C)</b>				
Drone (Raw)	-5.294	-3.778	-0.281	3.946
Outside	3.078	6.000	9.026	11.457
Drone (Adjusted by outside temperature)	-8.372	-9.779	-9.307	-7.512

Outside temperature in the experiment is the temperature recorded by a thermometer set 3.0 *m* apart from the house wall. “Drone temperature (Adjusted by outside temperature)” is defined as “Drone (Raw) temperature” minus “Outside temperature”.

## Appendix A

### Appendix A.1 *CH*-index

This appendix discusses the *CH*-index used in this paper. Occasionally, for a given number of the clusters,  $K$ , the *CH*-index is defined as

$$CH(K) \equiv \frac{B(K)/(K-1)}{W(K)/(n-K)}, \quad (\text{A1})$$

where  $n$  is the total number of houses. The within-cluster variation,  $W(K)$ , is given by  $W(K) \equiv \sum_{k=1}^K \sum_{i=1}^{n_k} (x_i - \bar{x}_k)^2$ , where  $n_k$  is the number of houses in cluster  $k$ ,  $x_i$  is the position of house  $i$ , and  $\bar{x}_k \equiv \frac{1}{n_k} \sum_{i=1}^{n_k} x_i$ . The between-cluster variation,  $B(K)$ , is given by  $B(K) \equiv \sum_{k=1}^K n_k (\bar{x}_k - \bar{x})^2$ , where  $\bar{x} \equiv \frac{1}{n} \sum_{i=1}^n x_i$ . Because our cluster analysis is not directly based on the locations of houses ( $x_i$ ) but on the distance between houses  $i$  and  $j$ ,  $d_{ij}$ , defined in (2), it is useful to rewrite the *CH*-index using  $d_{ij}$  and circumvent  $x_i$ ,  $\bar{x}$ , and  $\bar{x}_k$  appearing in the expression. Thus, we use the following version of the *CH*-index, which is equivalent to (A1),

$$CH(K) \equiv \frac{[T - W(K)]/(K-1)}{W(K)/(n-K)},$$

where  $T \equiv \frac{1}{n} \sum_{i=1}^n \sum_{j=i+1}^n d_{ij}^2$ , and  $W(K) = \sum_{k=1}^K \frac{1}{n_k} \sum_{i=1}^{n_k} \sum_{j=i+1}^{n_k} d_{ij}^2$ . This version of the *CH*-index is implemented by Halpin (2016).

### Appendix A.2 Segmentation in One-Dimensional Space

This appendix shows the results of grouping houses based on segmentation. In segmentation, each house is on a line that has a measurement. Figure A1a shows  $d_{1i}$ ,  $i \in \{2, \dots, 63\}$  on the vertical axis and the house ID on the horizontal axis.

[Figure A1 around here]

We consider a line starting from house 1. All houses are on the line and ordered by house ID. Stated differently, houses are ordered in terms of  $d_{1i}$  from small to large. By choosing  $\hat{K} - 1$  boundaries from 62 intervals to minimize the sum of the within-group sum of squared deviation from the group means, houses are optimally grouped into  $\hat{K}$  groups.<sup>A1</sup>

---

<sup>A1</sup>This procedure is implemented by a Stata user-written command “group1d.”

Next, we investigate the optimal number of groups using the elbow method. The vertical axis in Figure A1b is the sum of the within-group sum of squared deviation from the group mean for a given number of clusters (segments)  $\hat{K}$ . From Figure A1b,  $\hat{K} = 3$  or 4 appears to be the elbow. That is,  $\hat{K} = 3$  and 4 are candidates for the optimal number of segments. Inspection of Figure A1a reveals that the houses may be grouped into four groups rather than three: the first consists of houses 1 to 17, the second consists of houses 18 to 46, the third consists of houses 47 to 53, and the fourth consists of houses 53 to 63. This is the same classification as in the single-linkage clustering.

# Appendix B

## Appendix figures

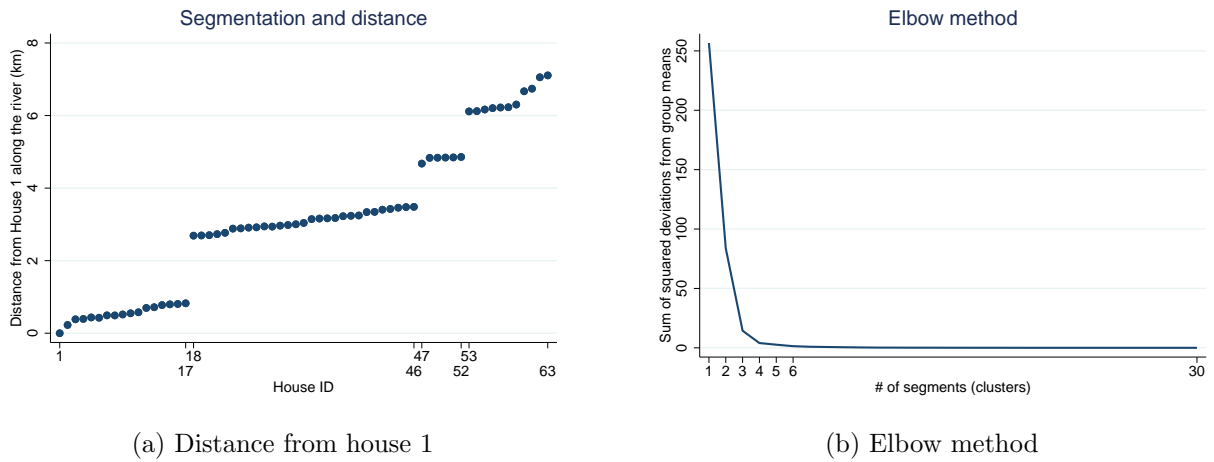


Figure A1: Segmentation and optimal number of segments

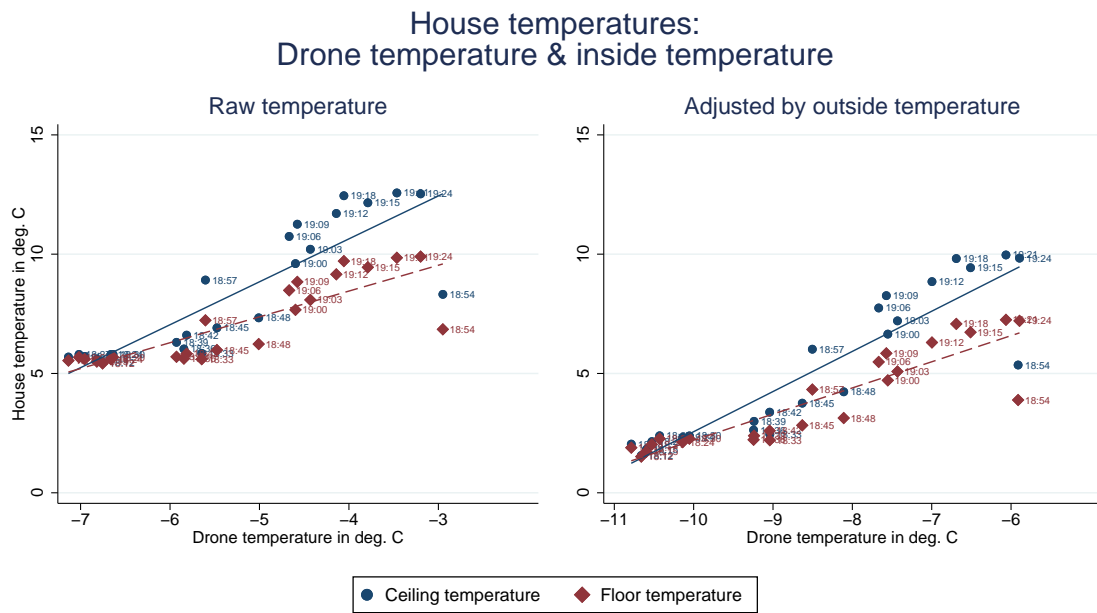


Figure A2: Comparison between drone and inside temperatures

In both panels of Figure A2, the navy solid line and red dashed line are linear fits of the ceiling temperature and floor temperature. In the right panel, “Drone temperature” is defined as “Drone temperature” minus “Outside temperature”, and “House temperature” is defined as “Inside temperature” minus “Outside temperature”. “Outside temperature” is the temperature 3m away from the house exterior wall.



## Online Appendix A

### More detailed explanation and additional discussion for Section 6

This online appendix section extensively discusses some of the robustness checks exhibited in Section 6.

#### Number of Supermarkets

In all specifications in Table OA4, the number of supermarkets near houses does not affect the living standards of homeless persons.

[Table OA4 around here]

This may be because our target area is highly urbanized, and there is an abundance of supermarkets, which leads to an insufficient variation in the number of supermarkets. Moreover, homeless persons may purchase food in supermarkets that sell items at discounted prices. The number of supermarkets alone does not capture which supermarkets homeless persons choose to buy food from at low prices.

#### Number of Scrap Firms

In Table OA5, the number of scrap firms has almost no impact on the living standards of homeless persons, although the sign of the scrap firm variable is positive, as expected.

[Table OA5 around here]

This insignificance may be caused by the closed transactions of used cans and metal scraps. Even though homeless persons earn money by selling the cans and metal they illegally collect to scrap firms, such informal transactions may be conducted with only a small number of scrap firms. In addition, information about which firms conduct informal deals with homeless persons is not open. Therefore, we cannot detect the effect of access to such illicit scrap buyers.

#### Distance to Nisshin Town

The coefficients of the distance to Nisshin Town in Table OA6 are positive, against our expectation of a negative sign for this variable, because better access (shorter distance) to Nisshin Town should lead to more job opportunities for homeless persons engaged in the construction sector, leading to higher living standards.

[Table OA6 around here]

The positive sign of the coefficient means that the farther from Nisshin Town homeless persons' houses are, the better off they are. There are two explanations for this unexpected sign.

First, homeless persons in the study area may not find daily jobs in Nisshin Town. Inexpensive hotels for homeless daily construction workers are located near Nisshin Town, and daily jobs offered around Nisshin Town are supplied to homeless persons staying in such hotels, not to those living in our study area. Homeless persons in our study area may not find job opportunities in Nisshin Town.

Second, there are gambling facilities located around Kawasaki Station, which is adjacent to Nisshin Town. Some of the homeless persons in Japan suffer from gambling addiction, and being close to an area with abundant gambling facilities may worsen homeless persons' situations because they waste money in an uneconomical manner. Thus, being close to Nisshin Town may negatively affect house temperatures.

### **Wind Speed Effect**

Similar to the calculation of the outside temperature, we calculate wind speed as follows:

$$\begin{aligned} & \text{WindSpeed}_{itd} \\ &= \frac{\text{WindSpeed}_{\text{Haneda},td} * \text{Distance}(\text{House}_i, \text{Fuchu})}{\text{Distance}(\text{House}_i, \text{Fuchu}) + \text{Distance}(\text{House}_i, \text{Haneda})} \\ &+ \frac{\text{WindSpeed}_{\text{Fuchu},td} * \text{Distance}(\text{House}_i, \text{Haneda})}{\text{Distance}(\text{House}_i, \text{Fuchu}) + \text{Distance}(\text{House}_i, \text{Haneda})}. \end{aligned}$$

In Table OA8, the wind speed variable is negative but insignificant in both specifications.

[Table OA8 around here]

This result is reasonable given the drone flight conditions. As drone flights are prohibited on windy days, and the flights to collect house temperature data were conducted under light wind, it is natural that the wind speed variable does not affect house temperatures.

### **Effect of Bridges**

This section explains how we excluded houses close to bridges. The distance between adjacent houses differs across pairs of houses, and the average distance between adjacent houses within a cluster also

differs across clusters. Thus, it is not appropriate to set the same distance to create a bridge buffer for all houses and clusters. Instead, we employ the following distance measure to create buffers around bridges:

$$d_{C(i)}^{\max} \equiv \max_{k \in C(i) \setminus \{\bar{k}_{C(i)}\}} d_{k,k+1}, \quad (\text{OA1})$$

where  $\bar{k}_{C(i)}$  is the maximum house ID in cluster  $C(i)$ , e.g.,  $\bar{k}_1 = 17$  for cluster 1,  $\bar{k}_2 = 46$  for cluster 2, and so on. In (OA1),  $d_{C(i)}^{\max}$  expresses the maximum distance between two adjacent houses belonging to the same cluster  $C(i)$ . The choice of the buffer (OA1) is explained as follows. By definition and the merging procedure of the cluster analysis, for every cluster  $C(i)$ , the distance between two arbitrarily chosen adjacent houses belonging to cluster  $C(i)$  is shorter than or equal to  $d_{C(i)}^{\max}$ . Therefore, if the distance between a bridge and the house closest to the bridge among houses in cluster  $C(i)$ , labeled as house  $i_{C(i)}^{\text{bridge}}$ , is longer than  $d_{C(i)}^{\max}$ , there is little possibility of houses located underneath the bridge. By contrast, if the distance between house  $i_{C(i)}^{\text{bridge}}$  and the bridge is shorter than  $d_{C(i)}^{\max}$ , there is a possibility that a house is hidden underneath the bridge. In such a case, the cluster to which house  $i_{C(i)}^{\text{bridge}}$  belongs may contain a larger number of houses than originally observed because of the hidden houses underneath the bridge. Thus, we drop such cluster(s) and repeat the analysis using the baseline model. Specifically, we run regressions by dropping cluster  $C(i)$  such that

$$\min_{k \in C(i)} d_{k,\text{bridge}} < d_{C(i)}^{\max}, \quad (\text{OA2})$$

where  $\min_{k \in C(i)} d_{k,\text{bridge}}$  is the distance between a bridge and the house closest to the bridge among houses in cluster  $C(i)$ .

We also conduct a less straightforward but similar analysis to the one stated above. Instead of dropping all houses belonging to the cluster satisfying (OA2), we drop houses that are sufficiently close to the bridge. Namely, we drop house  $i$ , a member of cluster  $C(i)$ , such that

$$d_{i,\text{bridge}} < d_{C(i)}^{\max}. \quad (\text{OA3})$$

Columns (1)–(4) in Table OA9 show the results when houses satisfying (OA3) are dropped, and columns (5)–(8) are the results when a cluster satisfying (OA2) is dropped.<sup>OA1</sup>

---

<sup>OA1</sup>In our dataset, only cluster 4 satisfies (OA2), so the number of clusters dropped from the analysis is one. Other clusters belong to the same administrative division, so the administrative fixed effect is not included in the model in Table OA9.

[Table OA9 around here]

### **Effect of Houses on the Opposite Shore**

We drop houses within 500 meters of each pedestrian bridge, which leaves 137 observations. In this robustness check, the house distribution on the shore of our study area (Kanagawa Prefecture) and that on the other side of the river (Tokyo side) are important. Unfortunately, we did not collect house location data on the opposite shore in 2019. To construct buffer lengths from pedestrian bridges, as we did in Section 6.7, house location data on the other side of the river, which we do not have, are indispensable. Therefore, we use a fixed value for the buffer length for all houses instead. As the river width in our study area is approximately 300–400 meters, we set the buffer length to 500 meters in this robustness check. In contrast to Section 6.7, we conduct a robustness check by dropping houses that are located near pedestrian bridges, but we cannot implement a robustness check by dropping clusters that contain at least one house that is within 500 meters of a pedestrian bridge. This is because the latter robustness check based on dropping clusters as a whole leaves only cluster 3, which contains six houses.

In the results displayed in columns (9)–(12) in Table OA9, the less significance of  $N(i)_{-i}$  and  $DN(i)_{-i}$  is found, although they are still significant at the 5% or 10% levels. This weaker significance may be partly because that the subsample of houses are imprecisely defined under the lack of the information about the house distribution on the other shore of the river.

## Online Appendix B

### Figures to online appendix



Figure OA1: Typical houses of homeless individuals in the study area

Figure OA1 is from an article “There is a struggle to find a safe place to sleep for the homeless” (in Japanese), Murata (2019) published in Toyo Keizai Online, <https://toyokeizai.net/articles/-/285068?page=7>, accessed on January 12, 2023.



Figure OA2: Toilet and tap in the bank area

Figure OA2 is a picture taken by the authors in the study area on February 3, 2020.

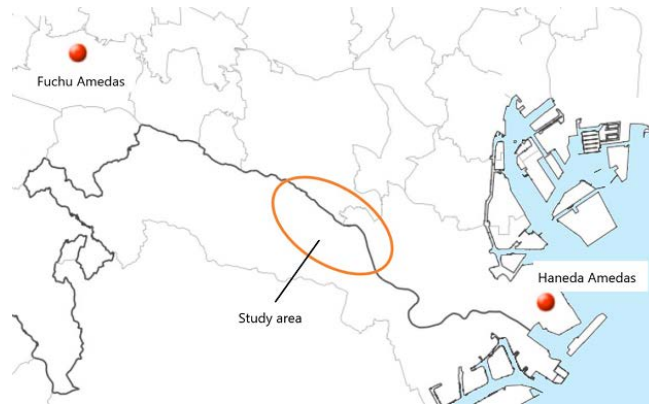


Figure OA3: Two AMeDAS stations and the study area

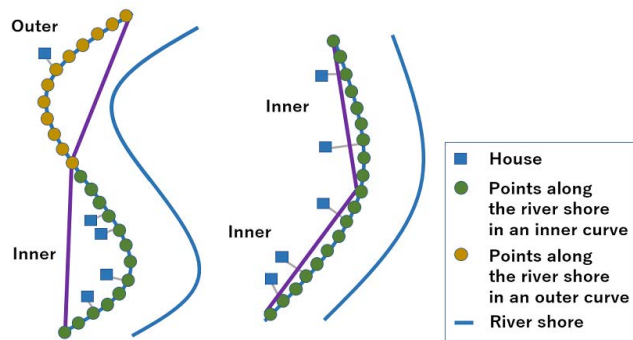


Figure OA4: Image of constructing the instrumental variable



(a) Exterior of replica house



(b) Interior of replica house



(c) Ceiling of replica house

### Figure OA5: Pictures of thermal experiment

Figure OA5a is a picture of the house taken by the authors in the thermal experiment on December 9, 2022. Figure OA5b is a picture inside the house taken by the authors in the thermal experiment on December 9, 2022. Two mobile volume batteries and small heaters were the heat origin. Figure OA5c is a picture of the ceiling of the house taken by the authors in the trial thermal experiment on February 28, 2022. Note that the house structure in the trial experiment is the same as in the thermal experiment conducted on December 9, 2022.

## Tables to online appendix

Table OA1: Data source

Variable	Source
House Temperature	Own collection and calculation
House location	Own collection
Outside temperature:	
Past temperature	Japan Meteorological Agency <a href="http://www.data.jma.go.jp/obd/stats/etrn/index.php">http://www.data.jma.go.jp/obd/stats/etrn/index.php</a>
Distance from the AMeDAS to houses	Own calculation
$N(i), N(i)_{-i}$	Own calculation from the house location data
$DN(i), DN(i)_{-i}$	Own calculation from the house location data
$ST(i), ST(i)_{-i}$	Own calculation from the house location and temperature data
$DST(i), DST(i)_{-i}$	Own calculation from the house location and temperature data
Inner/outer curve (1 if inner, 0 if outer)	Own calculation from Geospatial Information Authority of Japan (GIAJ) <a href="https://www.gsi.go.jp/ENGLISH/index.html">https://www.gsi.go.jp/ENGLISH/index.html</a>
Distance to toilet/tap ( $m$ )	Own calculation from the house location data and the GIAJ data
Forest coverage	Own collection and calculation
Grass coverage	Own collection and calculation
Distance to the river shore ( $m$ )	Own calculation from the house location data and the line data of the shore of Tama River provided by the National Land Numerical Information Download Service
Distance to Nisshin Town ( $km$ )	Own calculation from the house location data and the GIAJ data
House floor area	Own collection and calculation
Past wind speed:	
Past wind speed	Japan Meteorological Agency (JMA)
Distance from the AMeDAS to houses	Own calculation
Number of supermarkets ( $1km$ ):	
Data transformation	Own data transformation and calculation from the data of NTT Hello Page
Data transformation	Address matching service provided by Center for Spatial Information Science (CSIS), University of Tokyo <a href="http://newspat.csis.u-tokyo.ac.jp/geocode/">http://newspat.csis.u-tokyo.ac.jp/geocode/</a>
Number of scrap firms ( $2km$ ):	
Data transformation	Own data transformation and calculation from the data of NTT Hello Page
Data transformation	Address matching service provided by CSIS
Distance from bridges	Own calculation from the line data of the rail roads and roads provided by the National Land Numerical Information Download Service <a href="http://nlftp.mlit.go.jp/ksj-e/index.html">http://nlftp.mlit.go.jp/ksj-e/index.html</a>



Table OA2: Choice of  $ST(i)_{-i}$  and  $DST(i)_{-i}$  (max house temperature)

Model:	(1)	(2)	(3)	(4)	(5)	(6)	(7)	(8)
Sample:	RE	REIV	RE	REIV	RE	REIV	RE	REIV
Dependent variable:	Full				Houses with roofs fully visible			
	House Temperature (deg. C)							
$ST(i)_{-i}$ (max)	0.015*** (0.004)	0.050* (0.026)						
$DST(i)_{-i}$ (max)			0.027*** (0.008)	0.060* (0.032)				
$ST(i)_{-i}$ (max, roof fully visible)					0.027*** (0.010)	0.085** (0.034)		
$DST(i)_{-i}$ (max, roof fully visible)							0.047** (0.019)	0.104** (0.043)
Base control	Y	Y	Y	Y	Y	Y	Y	Y
Date FE	Y	Y	Y	Y	Y	Y	Y	Y
Administrative division FE	Y	Y	Y	Y	Y	Y	Y	Y
# of observations	160	160	160	160	111	111	111	111
Within R-sq	0.81		0.81		0.82		0.83	
Between R-sq	0.57		0.56		0.55		0.55	
Breusch and Pagan LM $\chi^2$	25.23		26.60		13.25		14.68	
[ p-val ]	0.00		0.00		0.00		0.00	
Sargan-Hansen stat. $\chi^2$	21.51		19.44		9.45		12.55	
[ p-val ]	0.00		0.00		0.02		0.01	
First stage								
Inner/outer curve (1 if inner, 0 if outer)		28.688*** (8.826)		23.953*** (7.253)		30.076*** (7.050)		24.572*** (5.926)
F-stat. (weak instrument)		10.57		10.91		18.20		17.19

Standard errors clustered by houses are in parentheses. Base control = Outside temperature, Distance to toilet/tap water, Forest and grass coverage (5-m buffers), Distance to the river shore.  $ST(i)_{-i}$ (max) and  $DST(i)_{-i}$ (max) are calculated based on the choice of the maximum temperature over the house polygon as the measure of the house temperature.

\*\*\* p<0.01, \*\* p<0.05, \* p<0.1

Table OA3: House Floor Area

Model:	(1)	(2)	(3)	(4)
	RE	REIV	RE	REIV
Dependent variable:	House Temperature (deg. C)			
$N(i)_{-i}$	0.094** (0.042)	0.215*** (0.076)		
$DN(i)_{-i}$			0.123** (0.058)	0.296*** (0.111)
House floor area ( $m^2$ )	-0.004 (0.028)	-0.035 (0.034)	-0.002 (0.027)	-0.034 (0.033)
Base control	Y	Y	Y	Y
Date FE	Y	Y	Y	Y
Administrative division FE	Y	Y	Y	Y
# of observations	160	160	160	160
Within R-sq	0.82		0.82	
Between R-sq	0.65		0.64	
Breusch and Pagan LM $\chi^2$	24.68		24.55	
[ p-val ]	0.00		0.00	
Sargan-Hansen stat. $\chi^2$	5.57		6.51	
[ p-val ]	0.06		0.04	
First stage				
Inner/outer curve (1 if inner, 0 if outer)		8.732*** (1.794)		6.353*** (1.430)
F-stat. (weak instrument)		23.70		19.73

Standard errors clustered by houses are in parentheses. Base control = Outside temperature, Distance to toilet/tap water, Forest and grass coverage (5-m buffers), Distance to the river shore.

\*\*\* p<0.01, \*\* p<0.05, \* p<0.1

Table OA4: Number of Supermarkets

Model:	(1)	(2)	(3)	(4)
	RE	REIV	RE	REIV
Dependent variable:	House Temperature (deg. C)			
$N(i)_{-i}$	0.093*** (0.035)	0.182*** (0.062)		
$DN(i)_{-i}$			0.122** (0.048)	0.251*** (0.087)
Number of supermarkets (1km)	-0.138 (0.117)	-0.144 (0.121)	-0.139 (0.117)	-0.146 (0.122)
Base control	Y	Y	Y	Y
Date FE	Y	Y	Y	Y
Administrative division FE	Y	Y	Y	Y
# of observations	160	160	160	160
Within R-sq	0.82		0.82	
Between R-sq	0.65		0.65	
Breusch and Pagan LM $\chi^2$	25.25		25.27	
[ p-val ]	0.00		0.00	
Sargan-Hansen stat. $\chi^2$	3.01		4.76	
[ p-val ]	0.22		0.09	
First stage				
Inner/outer curve (1 if inner, 0 if outer)		9.628*** (1.773)		7.001*** (1.398)
F-stat. (weak instrument)		29.49		25.09

Standard errors clustered by houses are in parentheses. Base control = Outside temperature, Distance to toilet/tap water, Forest and grass coverage (5-m buffers), Distance to the river shore. "Number of supermarkets" is the number of supermarkets within a 1-km radius from each house centroid.

\*\*\* p<0.01, \*\* p<0.05, \* p<0.1

Table OA5: Number of Scrap Firms

Model:	(1)	(2)	(3)	(4)
	RE	REIV	RE	REIV
Dependent variable:	House Temperature (deg. C)			
$N(i)_{-i}$	0.082** (0.034)	0.179*** (0.065)		
$DN(i)_{-i}$			0.108** (0.049)	0.247*** (0.092)
Number of scrap firms ( $2km$ )	0.113 (0.073)	0.088 (0.089)	0.117 (0.074)	0.093 (0.092)
Base control	Y	Y	Y	Y
Date FE	Y	Y	Y	Y
Administrative division FE	Y	Y	Y	Y
# of observations	160	160	160	160
Within R-sq	0.82		0.82	
Between R-sq	0.65		0.65	
Breusch and Pagan LM $\chi^2$	25.07		25.00	
[ p-val ]	0.00		0.00	
Sargan-Hansen stat. $\chi^2$	3.60		6.19	
[ p-val ]	0.17		0.05	
First stage				
Inner/outer curve (1 if inner, 0 if outer)		9.377*** (1.946)		6.837*** (1.555)
F-stat. (weak instrument)		23.22		19.32

Standard errors clustered by houses are in parentheses. Base control = Outside temperature, Distance to toilet/tap water, Forest and grass coverage ( $5-m$  buffers), Distance to the river shore. "Number of scrap firms" is the number of scrap firms within a  $2-km$  radius from each house centroid.

\*\*\*  $p < 0.01$ , \*\*  $p < 0.05$ , \*  $p < 0.1$

Table OA6: Distance to Nisshin Town

Model:	(1)	(2)	(3)	(4)
	RE	REIV	RE	REIV
Dependent variable:	House Temperature (deg. C)			
$N(i)_{-i}$	0.083** (0.033)	0.175*** (0.065)		
$DN(i)_{-i}$			0.113** (0.050)	0.236*** (0.088)
Distance to Nisshin Town ( $km$ )	0.380** (0.174)	0.319 (0.232)	0.409** (0.182)	0.377* (0.226)
Base control	Y	Y	Y	Y
Date FE	Y	Y	Y	Y
Administrative division FE	Y	Y	Y	Y
# of observations	160	160	160	160
Within R-sq	0.82		0.82	
Between R-sq	0.66		0.66	
Breusch and Pagan LM $\chi^2$	24.91		24.50	
[ p-val ]	0.00		0.00	
Sargan-Hansen stat. $\chi^2$	2.85		4.08	
[ p-val ]	0.24		0.13	
First stage				
Inner/outer curve (1 if inner, 0 if outer)		9.507*** (1.957)		7.052*** (1.519)
F-stat. (weak instrument)		23.60		21.57

Standard errors clustered by houses are in parentheses. Base control = Outside temperature, Distance to toilet/tap water, Forest and grass coverage (5- $m$  buffers), Distance to the river shore.

\*\*\*  $p < 0.01$ , \*\*  $p < 0.05$ , \*  $p < 0.1$

Table OA7: Vegetation Coverage

Model:	(1)	(2)	(3)	(4)	(5)	(6)	(7)	(8)
	RE	REIV	RE	REIV	RE	REIV	RE	REIV
Dependent variable:	House Temperature (deg. C)							
$N(i)_{-i}$	0.095** (0.042)	0.187*** (0.071)			0.111** (0.055)	0.203** (0.091)		
$DN(i)_{-i}$			0.130** (0.055)	0.256*** (0.099)			0.154** (0.071)	0.275** (0.125)
Forest coverage (10m, %)	0.070*** (0.023)	0.061*** (0.024)	0.070*** (0.023)	0.061*** (0.023)				
Grass coverage (10m, %)	0.031 (0.025)	0.022 (0.026)	0.033 (0.024)	0.024 (0.026)				
Forest coverage (15m, %)					0.030 (0.028)	0.014 (0.031)	0.030 (0.027)	0.016 (0.031)
Grass coverage (15m, %)					0.002 (0.026)	-0.014 (0.028)	0.003 (0.024)	-0.010 (0.027)
Base control excl. veg. cov.	Y	Y	Y	Y	Y	Y	Y	Y
Date FE	Y	Y	Y	Y	Y	Y	Y	Y
Administrative division FE	Y	Y	Y	Y	Y	Y	Y	Y
# of observations	160	160	160	160	160	160	160	160
Within R-sq	0.82		0.82		0.82		0.82	
Between R-sq	0.55		0.55		0.49		0.49	
Breusch and Pagan LM $\chi^2$	35.79		34.95		41.72		40.35	
[ p-val ]	0.00		0.00		0.00		0.00	
Sargan-Hansen stat. $\chi^2$	9.06		11.47		10.27		13.80	
[ p-val ]	0.01		0.00		0.01		0.00	
First stage								
Inner/outer curve (1 if inner, 0 if outer)		8.954*** (1.798)		6.534*** (1.456)		8.138*** (1.725)		6.006*** (1.451)
F-stat. (weak instrument)		24.79		20.15		22.26		17.14

Standard errors clustered by houses are in parentheses. Base control excl. veg. cov. = Outside temperature, Distance to toilet/tap water, Distance to the river shore.

\*\*\* p<0.01, \*\* p<0.05, \* p<0.1

Table OA8: Wind Speed

Model:	(1)	(2)	(3)	(4)
	RE	REIV	RE	REIV
Dependent variable:	House Temperature (deg. C)			
$N(i)_{-i}$	0.093** (0.039)	0.203*** (0.070)		
$DN(i)_{-i}$			0.122** (0.052)	0.278*** (0.100)
Wind speed ( $m/s$ )	-0.368 (0.692)	-0.459 (0.753)	-0.343 (0.681)	-0.419 (0.741)
Base control	Y	Y	Y	Y
Date FE	Y	Y	Y	Y
Administrative division FE	Y	Y	Y	Y
# of observations	160	160	160	160
Within R-sq	0.82		0.82	
Between R-sq	0.64		0.64	
Breusch and Pagan LM $\chi^2$	24.87		24.67	
[ p-val ]	0.00		0.00	
Sargan-Hansen stat. $\chi^2$	7.48		24.03	
[ p-val ]	0.06		0.00	
First stage				
Inner/outer curve (1 if inner, 0 if outer)		9.547*** (1.785)		6.957*** (1.407)
F-stat. (weak instrument)		28.59		24.44

Standard errors clustered by houses are in parentheses. Base control = Outside temperature, Distance to toilet/tap water, Forest and grass coverage (5-m buffers), Distance to the river shore.

\*\*\* p<0.01, \*\* p<0.05, \* p<0.1

Table OA9: Bridge Effects

	(1)	(2)	(3)	(4)	(5)	(6)	(7)	(8)	(9)	(10)	(11)	(12)
Sample:	Excl. houses near bridges				Excl. a cluster near bridges				Excl. houses near pedestrian bridges			
Model:	RE	REIV	RE	REIV	RE	REIV	RE	REIV	RE	REIV	RE	REIV
Dependent variable:	House Temperature (deg. C)											
$N(i)_{-i}$	0.089** (0.036)	0.172*** (0.064)			0.076** (0.035)	0.133** (0.059)			0.091* (0.052)	0.317* (0.167)		
$DN(i)_{-i}$			0.119** (0.049)	0.237*** (0.091)			0.109** (0.051)	0.181** (0.079)			0.124* (0.066)	0.324** (0.151)
Base control	Y	Y	Y	Y	Y	Y	Y	Y	Y	Y	Y	Y
Date FE	Y	Y	Y	Y	Y	Y	Y	Y	Y	Y	Y	Y
Administrative division FE	Y	Y	Y	Y	-	-	-	-	Y	Y	Y	Y
# of observations	142	142	142	142	136	136	136	136	137	137	137	137
Within R-sq	0.82		0.82		0.83		0.83		0.83		0.83	
Between R-sq	0.67		0.67		0.66		0.66		0.69		0.69	
Breusch and Pagan LM $\chi^2$	17.09		16.67		18.88		18.53		18.17		17.55	
[ p-val ]	0.00		0.00		0.00		0.00		0.00		0.00	
Sargan-Hansen stat. $\chi^2$	3.77		5.22		3.96		4.99		4.68		5.24	
[ p-val ]	0.15		0.07		0.14		0.08		0.10		0.07	
First stage												
Inner/outer curve (1 if inner, 0 if outer)		9.584*** (1.804)		6.958*** (1.459)		9.765*** (1.921)		7.220*** (1.531)		5.934** (2.556)		5.807*** (1.982)
F-stat. (weak instrument)		28.22		22.75		25.83		22.24		5.39		8.59

Standard errors clustered by houses are in parentheses. Base control = Outside temperature, Distance to toilet/tap water, Forest and grass coverage (5-m buffers), Distance to the river shore.

\*\*\* p<0.01, \*\* p<0.05, \* p<0.1